SUBJECT:	**FTS Pipeline Scientific Validation, Phase 1: Report of Module Testing**		
PREPARED BY:	**Ed Polehampton, Peter Davis-Imhof, Jean-Paul Baluteau**		
DOCUMENT No:	**SPIRE-RAL-DOC-003214**		
ISSUE:	**1.0**	**Date:**	**3rd November 2008**
APPROVED BY:		**Date:**	

Distribution

Jean-Paul Baluteau	LAM
Peter Davis-Imhof	Blue Sky Spectroscopy
Ed Polehampton	RAL
Peter Ade	Cardiff University
Trevor Fulton	Blue Sky Spectroscopy
Nanyao Lu	IPAC
David Naylor	University of Lethbridge
Giorgio Savini	Cardiff University
Christian Surace	LAM
Bruce Swinyard	RAL
Sarah Leeks	RAL
Chris Pearson	RAL
Tanya Lim	RAL
Matt Griffin	Cardiff University
Michael Pohlen	Cardiff University
Pasquale Panuzzo	CEA

Change Record

ISSUE	DATE	Changes
DRAFT 0.1	29 October 2008	
DRAFT 0.2	31 October 2008	Complete formatting and adding of reports
1.0	3 November 2008	Removed scripts in appendix – to be placed on Wiki

1 INTRODUCTION

1.1 The SPIRE FTS Validation Group

1.1.1 Group Membership

Coordinators:
Ed Polehampton (RAL)
Jean-Paul Baluteau (Marseille)
Peter Davis-Imhof (Blue Sky Spectroscopy)

Members:
Peter Ade (Cardiff)
Trevor Fulton (Blue Sky Spectroscopy)
Nanyao Lu (IPAC)
David Naylor (Lethbridge)
Giorgio Savini (Cardiff)
Bruce Swinyard (RAL)
Christian Surace (Marseille)

Cross-members (coordinating across all 4 groups):
Sarah Leeks (RAL)
Chris Pearson (RAL)

1.1.2 Objectives

The Objectives of the validation group are:

1. To ensure the pipeline conforms to the top-level documentation in terms of their overall architecture and detailed implementation.
2. To ensure that the developer documentation for individual modules conforms to the top-level documentation in terms of requirements and algorithms.
3. To verify that testing carried out at the developer module level is adequate and documented
4. To test the pipeline to validate the correct operation of individual modules and end-to-end systems.
5. To identify and initiate correction of errors or omissions in the pipeline documentation.
6. To identify and report errors in the module implementation and operation.
7. To document all results from the test phases.

The software test of pipeline modules aims to check:

- Consistency with the (already reviewed) top-level documents and module requirements
- Consistency with calibration file definitions (as described in the Pipeline Description Document)
- Correctness and clarity of implementation (i.e. algorithms used are correct and method clear)
- Commonality in use of symbols and terminology (i.e. inputs/outputs to each module use consistent terminology, algorithms use consistent symbols)
- Status of module-level testing (i.e. testing that has been carried out so far)

1.2 Structure of this Document

This document contains a review of the module level documentation for all modules in the spectrometer pipeline, and the final report of detailed testing of several specific modules. The module testing was carried out by splitting the FTS Validation Group into several sub-teams, divided by institute. Each team was allocated two modules to test. The final reports from these teams are given in Section 4.

1.3 Documents

1.3.1 Applicable Documents

Design Document	SPIRE Pipeline Design Document, version 0.1.0, 19 September 2008
Test Plan	SPIRE Pipeline Test Plan, version 0.1.0, 19 September 2008

1.3.2 Reference Documents

User Guide	SPIRE Pipeline User Guide, version 0.02, 18 September 2008
Chris' Document	SPIRE Pipeline Description (SPIRE-RAL-DOC-002437) Issue 1.0, 2 August 2008
Trevor's Document	SPIRE Spectrometer Pipeline Description (SPIRE-BSS-DOC-002966) Issue 1.1, 4 August 2008
Module Requirements	SPIRE Data Processing Pipeline Module Requirements (SPIRE-ICS-DOC-002998) Draft 1.4, 27 August 2008
Report on baseline subtraction	Removing the baseline of interferograms from the SPIRE imaging FTS (SPIRE-BSS-NOT-002996), Issue 1.0, 9 November 2007

2 List of Modules Tested

The following is a list of data processing tasks included in the FTS pipeline that were tested as part of Phase 1:

Processing task name	Sub-team carrying out test
First Level Deglitching	Marseille
Time-Domain Phase Correction	IPAC
Interferogram Creation	Cardiff/RAL
Interferogram Baseline Correction	Cardiff/RAL
Phase Correction	Marseille
Apodisation	Lethbridge
Fourier Transform of Interferogram	Lethbridge
Spectral Averaging	IPAC

3 Review of Pipeline Documents (Design & Test Plan)

Each module should have a section in the Pipeline Design Document and the Pipeline Test Plan. These documents are automatically generated from XML files that are included in the build with each module. The final compiled documents are also stored inside the build. The documents also contain a "common.xml" file which contains general introductory information about the module which is repeated in both Design Document and Test Plan.

At the moment not all of the modules in the pipeline have this documentation completed. The following table summarises the current situation.

Module	Common Info Section	Design Document	Test Plan
Compute BSM Angles	✓	4.2	
First Level Deglitching			
Removal of Electrical Crosstalk			
Clipping Correction			
Time-Domain Phase Correction			
Non-Linearity Correction	✓	3.8 (wrong title)	3.1
Temperature fluctuation correction			
Interferogram Creation	✓	3.4	3.5 (but empty)
SCAL and telescope correction	✓	3.7	3.8 (but empty)
Interferogram Baseline Correction	✓	3.2	3.3 (but empty)
Level 2 Deglitching	✓	3.5	3.6 (but empty)
Channel Fringe Correction			
Phase Correction	✓	3.6	3.7 (but empty)
Apodisation	✓	3.1	3.2 (but empty)
Fourier Transform of Interferogram	✓	3.3	3.4 (but empty)
Spectral Response Correction			
Flux Conversion			
Optical Crosstalk Removal			
Spectral Averaging			
Spatial Regridding			

3.1 General Comments

- We recommend that a general structure for the contents of the two documents be defined for all modules. Our suggestions are listed in the following two sections
- Title names of modules should agree with Trevor and Chris' documents
- Figures are not sized correctly and go off the page
- The recent update of the user guide has shown that the common information section was not useful. It should specifically be evaluated whether the common section is useful to the design document and test plan.

3.2 Pipeline Design Document

The content of the current Design Document is basically a description of the top level functionality of the module and repeats information already included in the top level documents.

We propose that the purpose of the Design Document is to describe the architectural design of the software module (by developers, for developers and software experts). We think that it should list the functionality and layout of the software (i.e. not list the maths, which is already described in the top level documents). It should define the data structures the software relies on, describe the structure of the software (e.g. class diagrams) and what the sequence of events is when the user calls the module, including all of the nitty gritty about what functions are called etc. It should not repeat detailed descriptions that are already included in the top level documents.

We propose that a set of standard section headings should be defined by Steve and Brian. These could include sections following the class structure of the module.

3.3 Pipeline Test Plan

None of the modules except the Non-linearity Correction have anything written in the Pipeline Test Plan. The Non-linearity Correction only has a brief list of 4 bullet points.

We propose that the purpose of the Test Plan is to list "verification" tests that check that the code meets the requirements in the Module Requirements Document. These are tests that are carried out in the automatic test harnesses that are run during the build process. There may also be additional testing carried out by hand before the module is uploaded to CVS which should also be described.

We propose that the Test Plan for a given module should be structured as follows:

- Test Harness
  Sub-sections for each test method within the class describing:
    - Applicable Requirements
      Via reference to the requirements document
    - Input data
      Its location in the build, how it is constructed (full details of any simulations) including enough detail to be able to reproduce the test
    - Test Description
    - Output data
    - Pass/Fail Criteria
      Including expected output values
- Manual Tests
  Details of further tests which have be carried out by hand, and the data that was used, and what exactly was tested and the (expected) results
    - Applicable Requirements
      Via reference to the requirements document
    - Input data
      Where it can be found and/or how it is constructed including enough detail to be able to reproduce the test
    - Test Description
    - Output data
    - Pass/Fail Criteria
      Including expected output values
    - Results
      Record of WHO executed the test WHEN and whether it passed or not
- Summary
  A summary matrix checking requirements against tests performed and identifying any requirements which have not been tested

The pipeline test plan should reference the modules requirements documents.

4 Software Testing of Modules

4.1 First Level Deglitching

Tested by Jean-Paul Baluteau and Dominique Benielli (Marseille).

As the module was designed to detect Dirac like glitches, only this kind of glitch were used to validate the task. At this stage ***only the glitch identification task*** has been tested. The glitch removal task will be tested later (during Phases 2 and 3).

4.1.1 Input Data

We used a real observation from PFM4, 0x300114C8, which provides 16 high resolution interferograms in quite dark conditions. Very few glitches were found during this observation.

OBSID	Date and Time	Mode	Number Scans	Source details
0x300114C8	27/11/06 18:04-18:29	H	16 High	CBB @ 6.7 K

In order to validate the task we made use of the record from 2 detectors (SSWD4 and SLWC3) for which no glitches were detected. Each record contains more than 100,000 samples.

300 glitches were added automatically to the recorded signal in the following way:

- all glitches have the same amplitude
- the first glitch is added at sample number 2000 and further glitches are added every 350 samples (this provides quite a random distribution of glitches with respect to the ZPD positions for the 16 scans)

Within this scheme we should be able to use the deglitching module to find:

- 18 glitches in the LowRes part (i.e. at positions less than 1250 µm away from ZPD)
- 62 glitches in the MedRes part (less than 5000 µm from ZPD)
- 300 glitches in the HighRes part

This should provide significant information regarding the percentage of glitches present that were actually detected for these three resolution modes.

4.1.2 Test Procedure

Four tests were made with glitch amplitudes of 5, 10, 20 and 40 times the rms signal noise (computed at the end of the record where the SMEC position is stable) with the default value for the three main parameters.

4.1.3 Test Results

Glitch detection results are as follows for the two pixels that were tested:

				Percentage		
SSWD4	Low	Medium	High	Low	Medium	High
5 x rms	0	2	17	0 %	3 %	6 %
10 x rms	0	28	201	0 %	45 %	67 %
20 x rms	4	45	278	22 %	73 %	93 %
40 x rms	9	53	291	50 %	85 %	97 %

SLWC3	Low	Medium	High	Percentage Low	Medium	High
5 x rms	0	0	2	0 %	0 %	1 %
10 x rms	0	3	102	0 %	5 %	34 %
20 x rms	0	9	186	0 %	15 %	62 %
40 x rms	0	12	204	0 %	19 %	68 %

These results are found to be close to our expectations. The large difference between the results for the two pixels can be understood taking into account the following two (conflicting) points:

- The true interferometric signal is much higher for SLWC3 than for SSWD4. The SNR (signal/amplitude of the central burst at ZPD compared to the rms noise) is 1600 for SLWC3 but only 120 for SSWD4. This means that it is harder to detect glitches for SLWC3 because the modulation due to real signal is higher (compared to the noise), and the glitches must be detected against a background that varies more than for SSWD4.
- As the signal frequency in SW detectors is twice the one in LW detectors, the ability to detect glitches is roughly a factor 2 worse for SW pixels than for LW ones. This is due to the higher slope in the interferogram modulation (i.e. frequency of modulations is higher for SW detectors).

Therefore we should expect a factor about 6 in glitch detection efficiency in favour of SSWD4 compared to SLWC3 which is roughly the kind of figure given in the results above.

4.1.4 Conclusions

Conclusion from these first tests:

- The ability to detect glitches is directly linked to the inverse of the maximum interferogram modulation (something which was expected).
- The conditions for in-flight observations (quite low interferometric signals after removal of telescope + SCAL emission) should be "fine" for a "good" glitch detection level. This is already quite encouraging.

4.1.5 Tests in progress

New test runs have been performed with the main module parameter values set to different values to the defaults. The analysis of these tests is in progress and should be included in the Phase 2 report.

4.1.6 Tests to be done

- collect information for "undetected" glitches
- try to establish a correlation of the glitch detection with the slope (signal difference between two adjacent samples) of the interferometric signal underlying each injected glitch

Tests to be done later are to make use of "real" glitches (at least a profile we think to be the one of expected glitches) instead of Dirac glitches once fine-tuning of main parameters is achieved

4.2 Time-Domain Phase Correction

Tested by Nanyao Lu (IPAC).

4.2.1 Input Data

Data from PFM4 and PFM5 were used as input. These are summarised below:

(A)

OBSID	Date and Time	Mode	Number Scans	Source details
0x300114D6	27/11/06 19:54-20:07	H	8 High	SCAL2 @ 9.17 K, CBB off
0x3001172F	06/12/06 15:29-15:42	H	8 High	CBB @ 13 K
0x300117A4	07/12/06 19:28-19:39	L	100 Low	Laser on SLWC3, aperture min

(B)

OBSID	Date and Time	Mode	Number Scans	Source details
0x30012497	05/03/07 17:31-17:53	M	32 Medium	SCAL2 @ 25.2 K

(C)

OBSID	Date and Time	Mode	Number Scans	Source details
0x300117FE	8/12/06 18:42-18:50	H	4 High	SCAL4 @ 67.9 K, Laser on SSWD3
0x30011802	8/12/06 19:36-19:47	H+L	2 High, 20 Low	SCAL4 @ 67.6 K, HBB warming up
0x30011800	8/12/06 19:11-19:24	M	20 Medium	SCAL4 @ 67.9 K, HBB warming up
0x30011801	8/12/06 19:26-19:33	L	40 Low	SCAL4 @ 67.6 K, HBB warming up

Level-0 telemetry data was downloaded from the RAL PFM4 and PFM5 databases. Calibration files were imported to the LocalStore using “cal_import”.

These tests were carried out using a MacBook Pro with 2G RAM (using Java 1.5).

4.2.2 General Test Procedures

1) Download the Level-0 data per OBSID from the PFM4 or PFM5 RAL database using obsExporter.

2) Process the data per OBSID basis using a Jython script called "test_TDPC.py". This script, which is a modified version of the pipeline script SOF1.py, only processes the data to the point where a spectrum is derived from each SMEC scan, just prior to the spectral phase correction. The script keeps two results, one with the Time Domain Phase Correction (TDPC) applied, one without this correction.

3) Compare the inverse and forward scan interferogram pairs between the case where the TDPC module is applied and that case where no TDPC is applied. The goal is to determine if the time delay between the reverse and forward scans is eliminated or at least significantly reduced when the TDPC is applied.

4) Compare the ratio of the imaginary part to the real part of the spectra derived at the end of this exercise between the case with TDPC applied and that without. The goal is to determine if this ratio is much reduced when TDPC is enabled.

4.2.3 Test Results

1) It was found that, if the TDPC module is not applied, there is significant time delay between a reverse and a forward scan. When the TDPC module is enabled, this time delay is pretty much eliminated. Figs. 1 through 4 demonstrate this result on some selected detector channels.

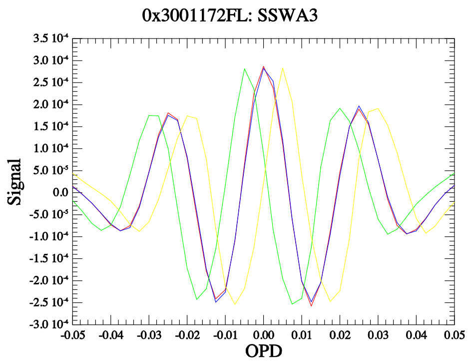

Figure 1: Individual interferograms near ZPD of channel SSWA3 from OBSID 300172F in PFM4. Reverse and forward scans without TDPC are shown in green and yellow, respectively, while their counterparts after TDPC correction are shown in red and blue, respectively.

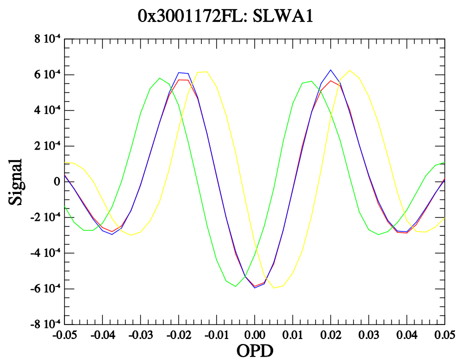

Figure 2: Individual interferograms near ZPD of channel SLWA1 from OBSID 300172F in PFM4. Reverse and forward scans without TDPC are shown in green and yellow, respectively, while their counterparts after TDPC correction are shown in red and blue, respectively.

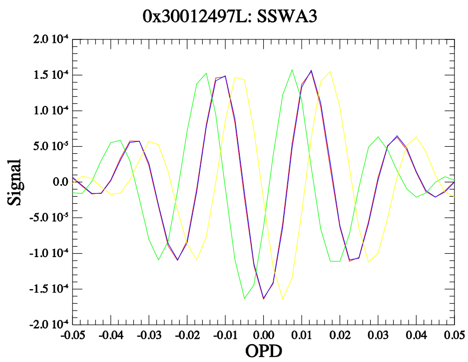

Figure 3: Same as in Fig. 1, but using the data from OBSID 30012497 in PFM5.

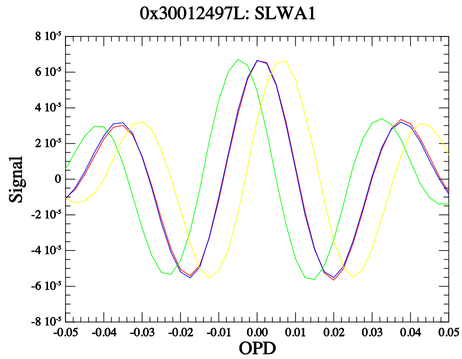

Figure 4: Same as in Fig. 2, but using the data from OBSID 30012497 in PFM5.

This result is true for all the test OBSIDs, except for those PFM4 tests in category (C) above. For test cases in data category (C), no obvious reduction of the time delay was observed after applying the TDPC module. It turned out that these test data have non-uniform sampling in time, especially the first sample point. This non-uniform sampling led to an incorrect estimate of sampling time interval in the TDPC module. Trevor has shown to me that this problem can be avoided by using the median time interval as the sampling time for the TDPC module.

2) After deriving a complex spectrum by Fourier Transform of an interferogram, the spectral phase, i.e. the ratios of the imaginary part to the real part within the passband is found to be much reduced when the TDPC module is applied. Figs. 5-8 show some examples of this result. In general, the reduction of the imaginary part of the derived spectra is on the order of a factor of 10 or more when the TDPC module is applied in the data reduction.

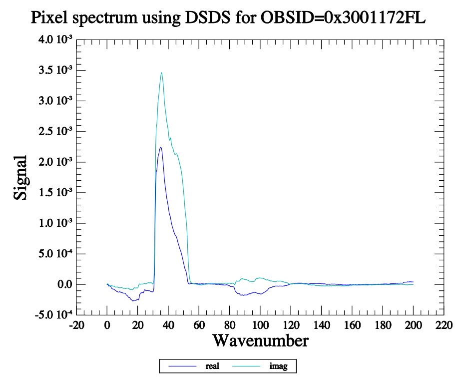

Figure 5: Real and imaginary parts of the spectrum of SSWA3 in OBSID 3001172F without TDPC.

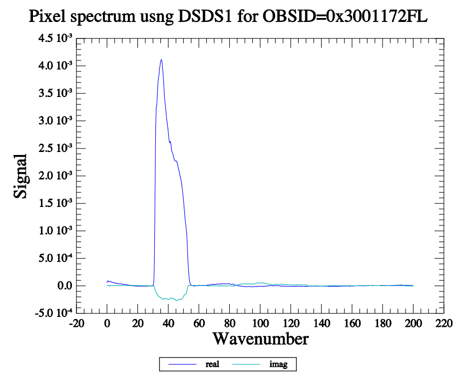

Figure 6: Same as Fig. 5, but after the TDPC.

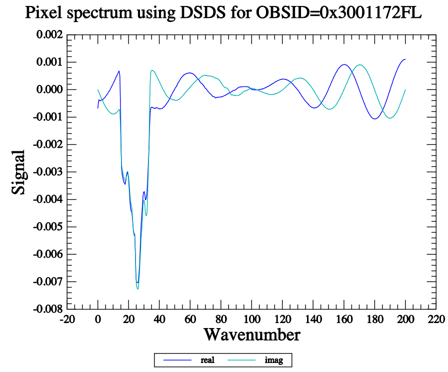

Figure 7: Real and imaginary parts of the spectrum of SLWA1 in OBSID 3001172F without TDPC.

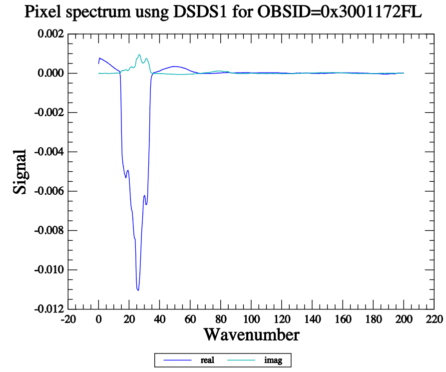

Figure 8: Same as Fig. 7, but after TDPC.

My conclusion is that the TDPC module, as implemented now, works very well. The only major caveat is to modify it to accommodate the non-uniform sampling within a BBID, see SPR-0952.

4.2.4 General Comments on the Pipeline Script SOF1.py

(1) The "bbtype" in the SOF1 script works only on AOT type OBSID. One needs to modify it in other cases:

For example,

```
# if AOT use the following:
if bbtype == 0xa106:
# ==> this works on, e.g., 300117FE
# if not AOT, use the following:
if bbtype == 0x8203:
# ==> this works on, e.g., 3001172F
# If neither above failed, just simply use:
if count == 0:
# ==> this works on, e.g., 30012497
```

(2) The following doesn't allow me to set plot =1:

```
# cannot change plot to 1 in the above Dialog.
plot=inputs.plot
```

(3) plotSpectrum (sds, name, title) will not work after spectra are averaged.

4.3 Interferogram Creation

Tested by Giorgio Savini (Cardiff) and Ed Polehampton (RAL).

The purpose of this module is to take the timeline detector data, and SMEC data, convert MPD to OPD, and interpolate them onto an OPD grid with constant step size.

A calibration file is used to supply positions of ZPD, and scaling factors from MPD to OPD.

4.3.1 Input Data

Real data observations from PFM4 were used as input. These are summarised below:

OBSID	Date and Time	Mode	Number Scans	Source details
0x300117FE	8/12/06 18:42-18:50	H	4 High	SCAL4 @ 67.9 K, Laser on SSWD3
0x30011800	8/12/06 19:11-19:24	M	20 Medium	SCAL4 @ 67.9 K, HBB warming up
0x30011801	8/12/06 19:26-19:33	L	40 Low	SCAL4 @ 67.6 K, HBB warming up

In order to process these for input to the module, we used the obsExporter tool to obtain Level-0.5 data from the database in a pool. We then ran the first step of the pipeline (Time Domain Phase Correction) to align the ZPD in forward and reverse scans.

We saved the input products and output products from the module as FITS files and carried out further analysis using both IDL and HIPE.

4.3.2 Test Procedure

We aimed to test the following points:

- Interpolation to OPD correct
- Interferogram has expected sampling
- Interferogram covers the correct OPD range for the spectral resolution used
- Obliquity effect correctly taken into account

4.3.2.1 Interpolation of detector data onto OPD scale

In order to test the correct interpolation in the module, we carried out the first step of the process in IDL to interpolate the SMEC position onto the timeline of the detector data. This allowed us to compare the detector data vs. SMEC position with the final result of the module and verify that the detector data was not changed at all by the module.

In order to compare the two we applied the conversion from MPD to OPD to our interpolated position scale, i.e. OPD=*f* (MPD-ZPD), using the value of ZPD from the calibration file, SCalSpecSmecZpd. Figure 9 shows the result for detector SSWC1, and confirms that the interpolated detector values using IDL agree with the final interferogram in the SDI output of the module. The only difference is that the grid of OPD in the module output has also been put onto a uniform grid in OPD.

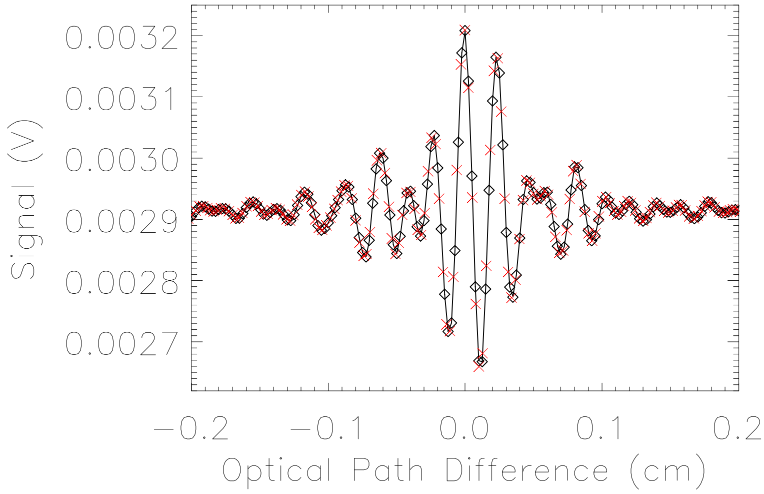

Fig 9: A comparison of the output of the Create Interferogram module for detector SSWC1 (OBSID 300117FE, scan 0001) with an interpolation of the input data using IDL. The solid line with diamonds is the module output, and the red crosses are the IDL values.

In carrying out this test we noticed that the scans are numbered in reverse order with respect to time. This means that the first scan in the SDT does not correspond to scan 0001 in the SDI product. Trevor explained that the numbering is determined from the housekeeping SCANS parameter. Ken explained that this takes the number of requested scans and counts down from that number to zero. But is this what people will expect? – it makes it harder to compare scans from the input and output of this task.

4.3.2.2 Investigation of regular grid parameters

We examined the final grid of OPD used in the output of the module. The spacing in OPD is constant with a 25 µm step. We tried to confirm this value by calculation, examining the SDT and SMECT for OBSID 300117FE.

Sampling frequency of detector timeline:
`1/median(sdt.sampletime-shift(sdt.sampletime,1))` = **75.12 Hz**

Step in SMEC position:
```
median(abs((smect.encodercoarse+smect.encoderfine)- $
    shift((smect.encodercoarse+smect.encoderfine),-1))) = 0.0002093 cm
```

Sampling frequency of SMEC timeline:
`1/median(smect.sampletime-shift(smect.sampletime,1))` = **237.46 Hz**

So the SMEC speed = 0.0002093 × 237.46 = **0.0497 cm/s**

In Trevor's document, the step in OPD is determined by 4 × SMEC speed/sampling freq

4 × 0.0497/75.12 = **26.46 µm**

This should then be rounded down to the nearest integer in units of microns, but that still gives us a discrepancy between the observed 25 µm step and our calculated 26 µm.

We noted that although the OPD vectors had consistent length and values for all the scans from one particular detector, that some detectors had an extra point. This leads to different vector sizes for different detectors (although all having a consistent step in OPD of 25 µm).

4.3.2.3 OPD range of interferogram

We tested the expected OPD range in the final interferogram. We noted that due to the differing length of the vectors for different detectors (by one point), and the fact that the ZPD position is different for different detectors, that there are small differences in the minimum and maximum OPD for different detectors. This means that different detectors will have slightly different intrinsic spectral resolutions.

Figure 10 shows plots of the start and end OPD position for observation 0x300117FE. This plot shows that although there is a wide range in start and end positions for the scan, the length is always within one point (25 µm) for all detectors.

The minimum OPD ranges to obtain the required spectral resolution for L, M and H modes can be calculated from,

$$L = \frac{1}{2\Delta\sigma}$$

where Δσ is the spectral resolution.

There is supposed to be an additional 250 µm added to the length of travel in MPD to allow for the SMEC coming up to speed. As far as we know this is not removed by the task so may be included in the final OPD range. This is an extra 0.1 cm.

Mode	Spectral resolution	Minimum length OPD	Final OPD length required
Low	1.0 cm^{-1}	0.5 cm	0.6 cm
Medium	0.25 cm^{-1}	2.0 cm	2.1 cm
High	0.04 cm^{-1}	12.5 cm	12.6 cm

For Low and Medium resolution scans, the actual OPD range should be symmetric about ZPD. For high resolution, the range is not symmetric and only the end point of the scan in OPD can be compared with the expected values in the previous table. The actual values we observe in the test observations for the range of start and end OPD are (the range is from different detectors):

Mode	OBSID	OPD start (cm)	OPD end (cm)
Low	0x30011801	-0.7175 to -0.7000	0.7025 to 0.72000
Medium	0x30011800	-3.1125 to -3.0950	3.1225 to 3.1400
High	0x300117FE	-2.8625 to -2.8450	12.6525 to 12.670

These ranges imply that all data available is used – i.e. that even though extra time was allowed for the SMEC coming up to speed, this is all included together in the final interferogram. The start and end positions imply the following spectral resolutions can be achieved:

Mode	OBSID	Spectral Resolution	Advertised Resolution
Low	0x30011801	0.694 - 0.714 cm^{-1}	1.0 cm^{-1}
Medium	0x30011800	0.159 - 0.162 cm^{-1}	0.25 cm^{-1}
High	0x300117FE	0.0395 cm^{-1}	0.04 cm^{-1}

Note that these data were test observations, rather than real AOTs and we are not sure what the actual commanded ranges were compared to the standard AOT values. The OPD ranges seen above are consistent with the commanded MPD ranges included in the housekeeping data for these observations, except for the high resolution observation which has an OPD range here slightly lower than implied by the housekeeping MPD values.

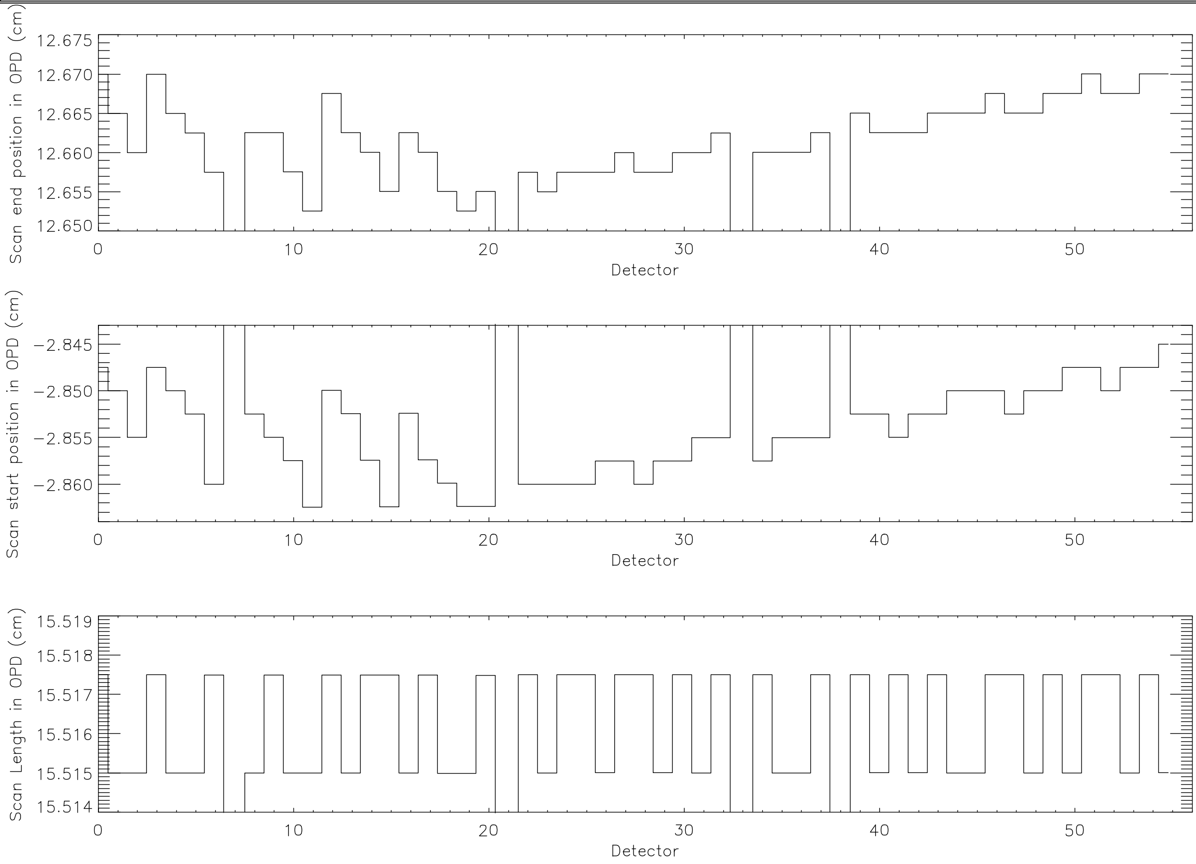

Figure 10: Plot showing the start and end positions of the OPD vector for scan number 0001 in observation 300117FE (high resolution). The x-axis shows all of the detectors (in alphabetical order from SLWA1 to SSW G4). Note that there are 4 dead detectors that were excluded from the SDI product (hence the 4 points where the plot goes off scale).

4.3.2.4 Obliquity factor

In the conversion from MPD to OPD the factor, *f*, is supposed to correct for the obliquity effect,

$$OPD = f\left(MPD - ZPD\right)$$

This factor is contained in the SCalSpecSmecStepFactor calibration file. Currently all values are set to the nominal 4.0. In order to test the application of this factor, we examined the interferograms for different pixels using the high resolution observation 0x300117FE. In this observation the laser was centred on detector SSWD3, but was still detected on SSWD4 (centre of the array) and SSWD2 near the edge.

With no correction for the off centre detectors, the signature of the laser in the interferogram is stretched out. This means that the peaks and troughs in SSWD2 appear at larger OPD values than in SSWD3. This is shown in Fig 11. The factor, f, should correct this by multiplying the OPD scale of SSWD2 by a number lower than 4.0. By comparing the peaks in the interferogram, we calculated that this factor should be 3.9976.

We modified the calibration product to change the entry for SSWD2 from 4.0 to 3.9976. We then re-ran the module, and examined the output interferogram. This is shown in green in Fig 11 and does match up with the peaks in the interferogram from SSWD3. This shows that the obliquity correction factors are applied correctly in the module.

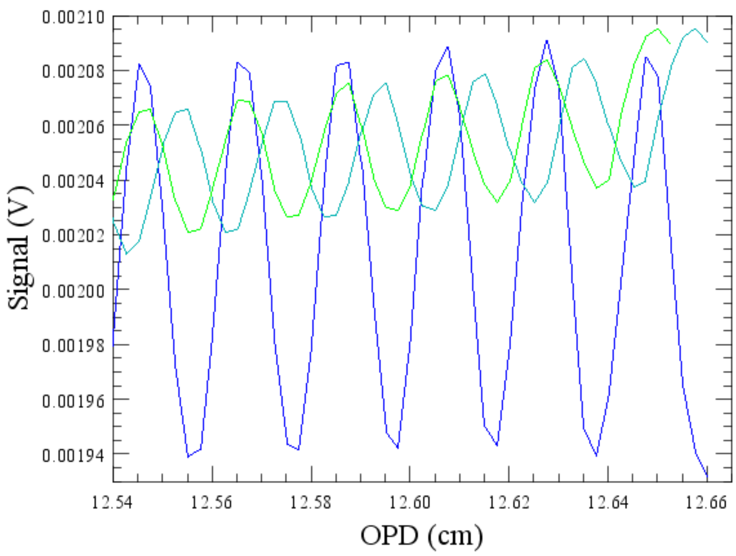

Figure 11: Comparison of the high OPD region of the interferogram for detector SSWD3 (dark blue) for observation 300117FE. The data from detector SSWD2 are shown in light blue. The corrected data for SSWD2 are shown in green.

4.3.3 Conclusions, Recommendations & Comments

A summary of the results of the tests performed are:

Test	Result
Interpolation to OPD correct	Pass
Interferogram has expected sampling	Pass
Interferogram covers the correct OPD range for the spectral resolution used	Pass
Obliquity effect correctly taken into account	Pass

All the tests passed, although we noted the following points:

- Scans are numbered in reverse order with respect to time
- OPD grid for different detectors have differing lengths (by 1 point)
- OPD step could not be reproduced using the algorithm in the document

It would make more sense for astronomers if the scan numbering was changed to match time order, or otherwise described clearly in the user documentation.

The difference in length of OPD grids for different detectors does not seem to cause a problem, but it could be mentioned in the user documentation that different detectors have slightly different intrinsic spectral resolutions (also due to the differing ZPD positions for each detector), as this would be important if someone wanted to co-add data from different detectors together (e.g. to increase the signal to noise in the spectrum).

The calculation that we did to determine the OPD interval may be wrong – this should be checked and if necessary the description updated in the document describing what is done.

4.4 Interferogram Baseline Correction

Tested by Giorgio Savini (Cardiff) and Ed Polehampton (RAL).

4.4.1 Input Data

The input data used was the same as used for the Create Interferogram module tests, i.e.,

OBSID	Date and Time	Mode	Number Scans	Source details
0x300117FE	8/12/06 18:42-18:50	H	4 High	SCAL4 @ 67.9 K, Laser on SSWD3
0x30011800	8/12/06 19:11-19:24	M	20 Medium	SCAL4 @ 67.9 K, HBB warming up
0x30011801	8/12/06 19:26-19:33	L	40 Low	SCAL4 @ 67.6 K, HBB warming up

We ran the module in HIPE using the output of the Create Interferogram task as the input. We saved the results as FITS files, and carried out further analysis in IDL.

4.4.2 Test Procedure

We aimed to test the following points:

- That when no baseline is present in the input, it is not changed in the output
- Check the optimum parameters
- Check baseline correction for all spectral resolution modes

4.4.2.1 General points

In checking this module in HIPE, we often had to perform operations such as subtracting the output product from the input product (to get the fitted baseline). We noted that there is no operator overloading defined for SDI products to allow them to be subtracted directly, but each scan had to be subtracted manually. It would be useful to overload the arithmetic operators for these products such that the result of an operation on two SDI products of the same size is applied to all scans and all detectors.

We noted that in order to compare the input and output of this task in HIPE, we had to save the input as a FITS file and re-read it in because the task modified both the input **and** output variables. We think this will be extremely confusing for Interactive Analysis users, and if it is required for memory reasons, should be explained very carefully in the User Manual.

4.4.2.2 Test when no baseline present

In order to test that an interferogram with no baseline present remains unchanged in the output of the module, we carried out a test where we ran the module once to remove the baseline. We then put the resulting baseline subtracted interferogram back into the task to see whether it was altered in a second pass through the module.

We tested this using both polynomial fits and Fourier components on the high resolution observation 300117FE.

For a polynomial baseline, the second fit did not change the output significantly (the second baseline fit was always less than 10^{-5} times the actual signal – i.e. the change in the signal due to subtracting the second baseline was less than 0.001%).

For the Fourier transform method, the second pass through the module does fit a significant baseline which changes the modulation away from ZPD (see Figure 12).

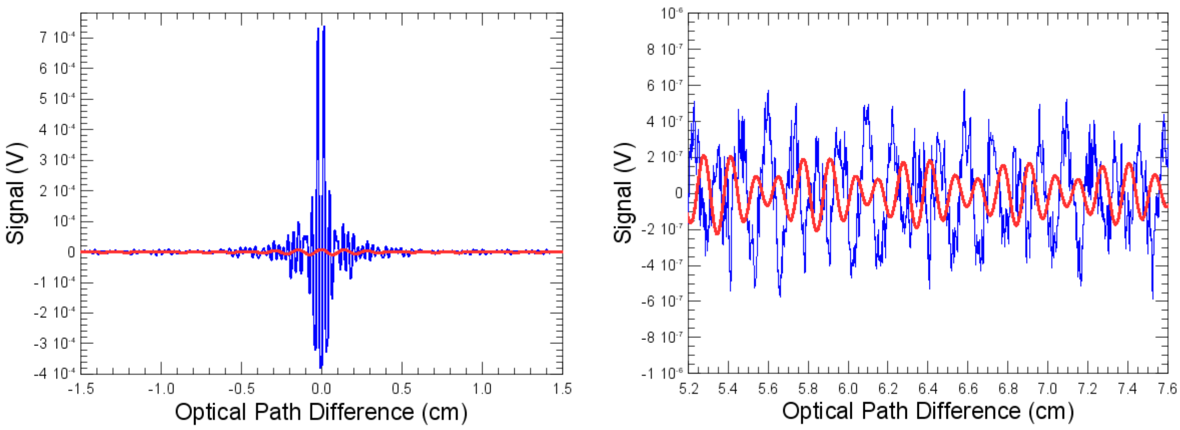

Figure 12: The results of performing a second baseline fit using the Fourier Component method with cutoff of 4 cm^{-1} for pixel SLWC5 from observation 300117FE (original data in blue, fit in red). The left panel shows the region near ZPD and the right panel shows the region away from ZPD.

4.4.2.3 Optimum parameters

We carried out a few tests with different polynomial degrees, and different Fourier component cutoff values. We found nothing new to add to the report on baseline subtraction by Blue Sky Spectroscopy, except to note that we obtained marginally better results for the polynomial fit when the region around ZPD was masked out.

We examined the difference between the polynomial fit and Fourier component fits with their default parameters (4th order, or 4 cm^{-1} cutoff) and agreed with the conclusion that the polynomial fit should be the baseline for the automatic pipeline. This is because the Fourier component fit has a larger effect on the signal at ZPD, and should therefore probably only be used with care in Interactive Analysis – see Figure 13.

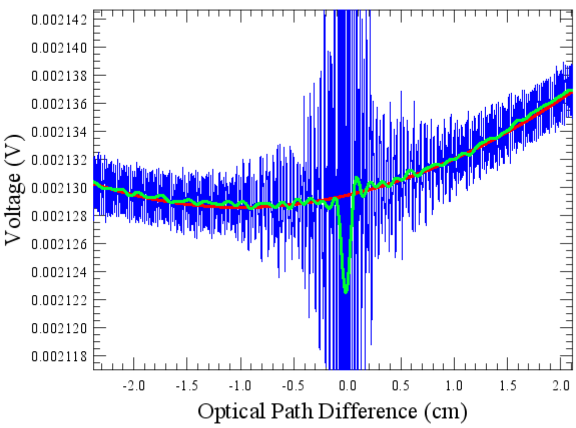

Figure 13: The polynomial fit (red) compared to the Fourier component fit (green) around ZPD for SSWD2 in the high resolution observation 300117FE.

It is noted in the baseline subtraction report that there is a problem with clipped interferograms (Section 3.1.2 of that report). We found that as well as interferograms that are clipped at ZPD, there were also instances of clipping of the region far from ZPD. In the high resolution observation 300117FE, the detectors affected are SSWD1 and SSWB1. The resulting fit is shown in Figure 14. We recommend that the clipped region be masked out in any polynomial fit.

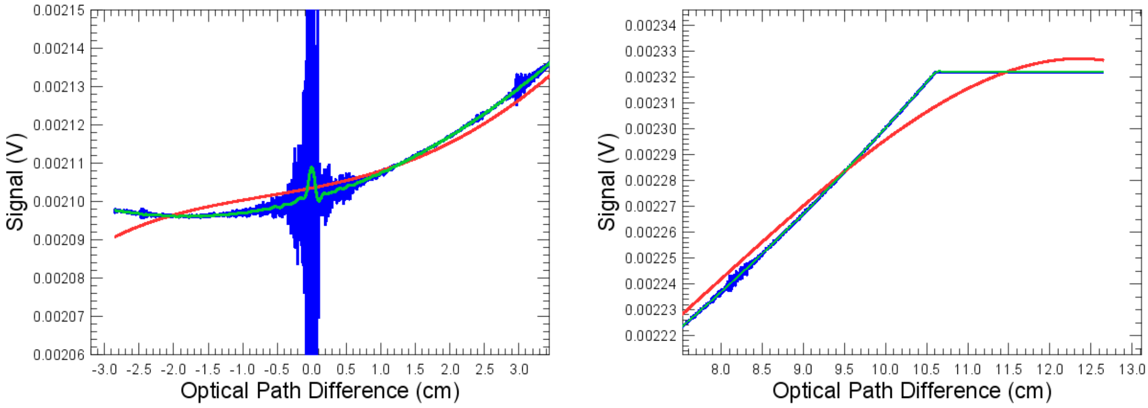

Figure 14: Results of a polynomial and Fourier component fit on detector SSWD1 in the high resolution observation 300117FE. The region far from ZPD is clipped and this causes a miss-fit of the polynomial at both ends of the interferogram. The original data are in blue, the polynomial fit in red, and the Fourier component fit in green.

4.4.2.4 Low and Medium resolution observations

The results for the high resolution observation apply equally well to the medium resolution observation.

The low resolution observation, 30011801 did not have any visible baseline as the scan range is restricted enough around ZPD that the effect of vignetting is not seen. This provides another reason to use the polynomial fit in the standard pipeline as it does not alter the low resolution scans. The Fourier component fit, however, does make some correction around ZPD in the low resolution scans.

4.4.3 Conclusions

We noted two general recommendations:
- Arithmetic operator overloading could be considered for SDI products
- The fact the input to the baseline module is also changed should be clearly documented

The conclusions of the testing are:
- Polynomial fits of 4th order should be maintained in the standard pipeline.
- To improve these fits, the region around ZPD could be masked out, and also any clipped points could be ignored in the fit.

We noted in general that there was little effect from the baseline fit on the total power in the spectrum, even when it appeared visibly that there seemed to be a big difference in the fit. However, we did not get time to carry out a thorough test of the effect on the total power to extend what had already been done in the report on baseline subtraction.

4.5 Phase Correction

Tested by Jean-Paul Baluteau and Dominique Benielli (Marseille).

4.5.1 Input Data

PFM4

OBSID	Date and Time	Mode	Number Scans	Source details
0x300114CB	27/11/06 18:39-18:42	L	16 Low	SCal and CBB off
0x300114D0	27/11/06 19:24-19:27	L	16 Low	SCal off and CBB @ 9K
0x300114ED	27/11/06 22:30-22:33	L	16 Low	SCal4 @ 20K and CBB off
0x300114CF	27/11/06 19:18-19:24	M	16 Medium	SCal off and CBB @ 9K

PFM5

OBSID	Date and Time	Mode	Number Scans	Source details
0x30012495	05/03/07 16:56:00	M	2 Medium	Dark conditions

4.5.2 Test Procedure

For each observational run the spectral "residual" phase was computed for the module input data and for the module output data. “Phase” here is just the ratio of spectral imaginary over real parts. The output phase was then compared to the input phase. For convenience only two pixels were considered: i.e. SLWC3 and SSWD4 as illustrative of the majority of pixels in the two arrays.

4.5.2.1 Low Res observations

PFM4:30014CB run: this is not a true Low Resolution AOT. The input interferogram is sampled from OPD -0.3425 cm to +0.4600 cm (with 0.0025 cm step) instead of having a range of +/- 0.5 cm.

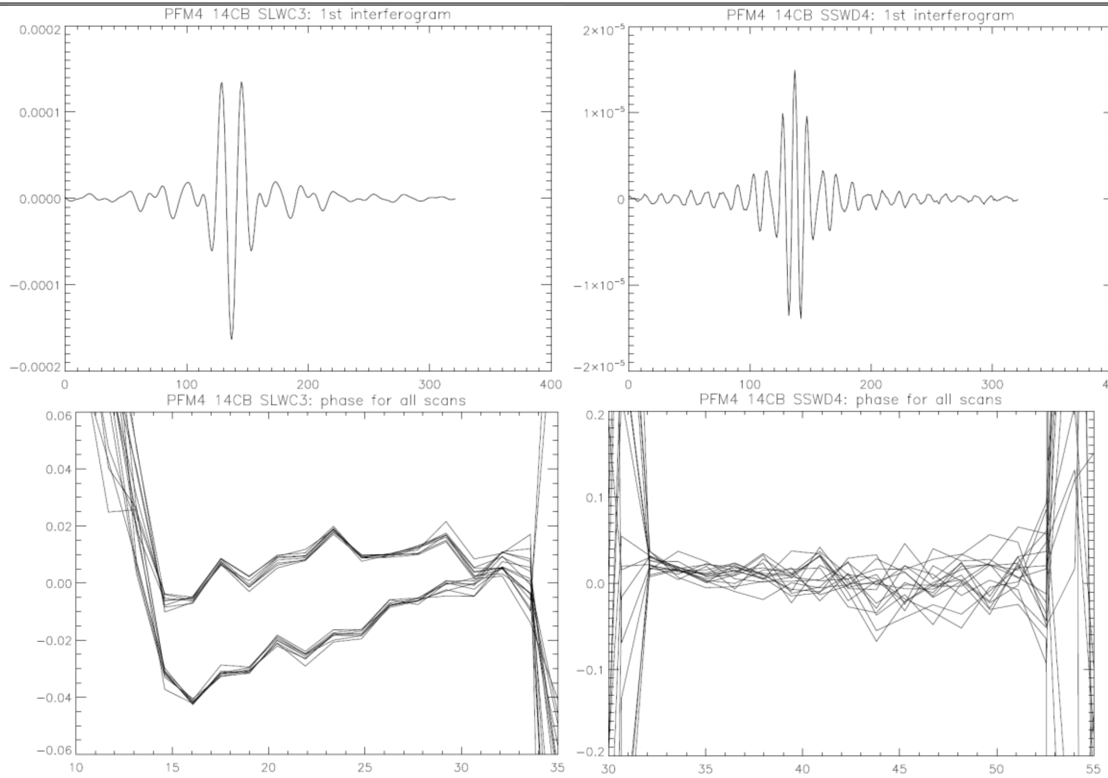

Figure 15: Input interferograms and spectral phases for the 2 pixels (SLWC3 & SSWD4).

Note the different residual phase aspect from forward and reverse scans (at least for SLWC3) and the apparent highly structured shape of the residual phases.

Note also that the interferometric signal in the output data seems to be N times (N = total number of samples for the FFT) higher than the one in the input data (see below for an example): one should expect the same signal strength (?). As the resolution is much lower than expected no quantitative useful results can be obtained from this run. Same conclusion for the two other Low Res runs 30014D0 and 30014ED.

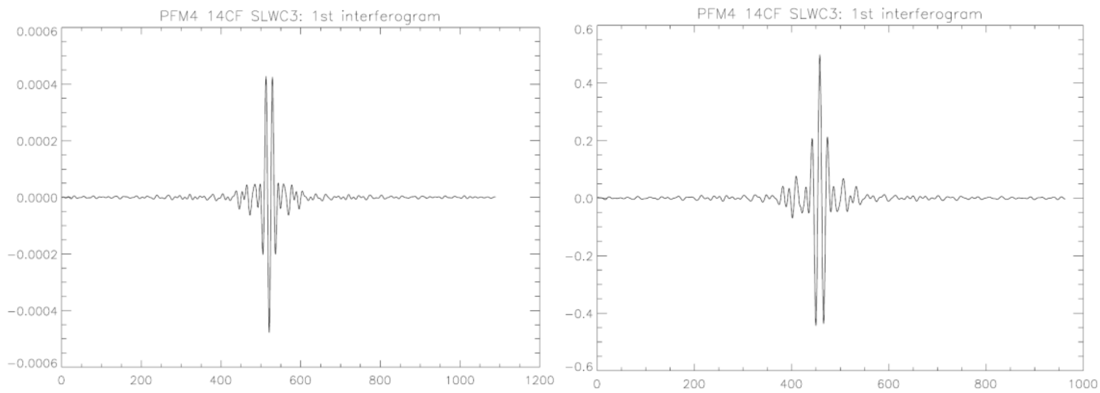

Figure 16: Interferogram before and after phase correction.

4.5.2.2 Medium Res observations

PFM5 3002495 run: again this is not a true Medium Resolution AOT. The input interferograms are sampled from OPD -3.0625 to +3.0675 cm instead of +/- 2.0 cm.

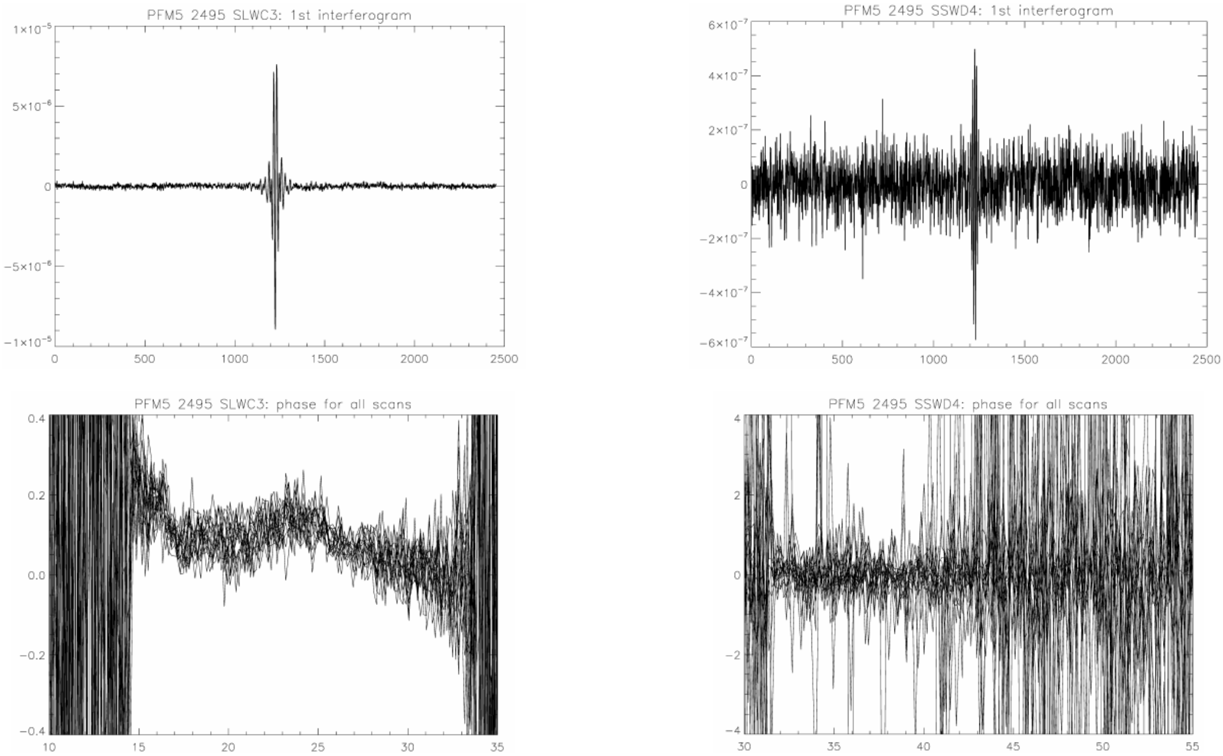

Figure 17: Input interferograms and spectral phases for the 2 investigated pixels.

As this run is from very "dark" conditions (the darkest recorded within the PFMs campaign), the interferometric signals are very low, especially for SSWD4, therefore the residual phase is very noisy: however, since the run has 32 scans we can see again some structure appearing from the noise. There is no apparent residual phase in SSWD2 but still a clear one in SLWC3. In this last case, there is no significant difference between phases from forward and reverse scans, but still some structure can be seen.

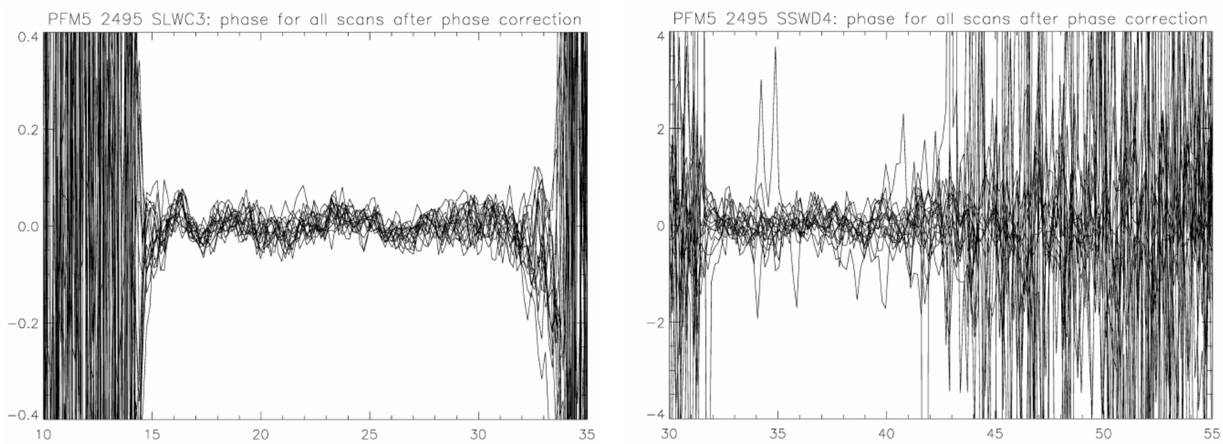

Figure 18: Residual phases in the output data.

There is effectively a great and significant reduction of the residual phase for SLWC3, and now the phase "structure" can be more clearly seen. As the signal for SSWD4 is very faint, a phase reduction, if any, is very difficult to appreciate within the high noise level. Again note that the interferometric signals are N times higher in output data compared to input data (as already seen for the LR data). In fact this is a common feature for all the runs investigated here.

PFM4 30014CF run: again this is not a true Medium Resolution AOT. The input interferograms are sampled from OPD -1.3025 to +1.4200 cm instead of +/- 2.0 cm, and the output interferograms are from -1.1459 to +1.2625 cm.

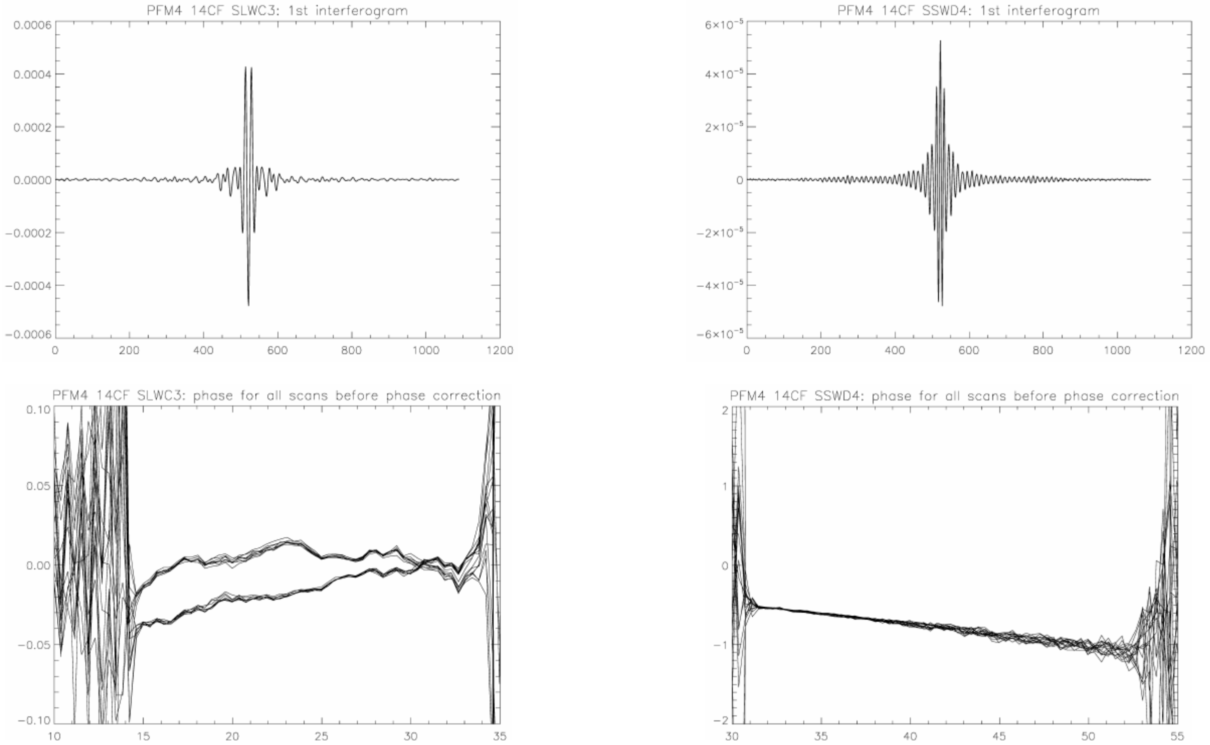

Figure 19: Input interferograms and spectral phases for the 2 investigated pixels

The results are close to what were seen for the LR run 30014CB (see above) and the same conclusions may apply.

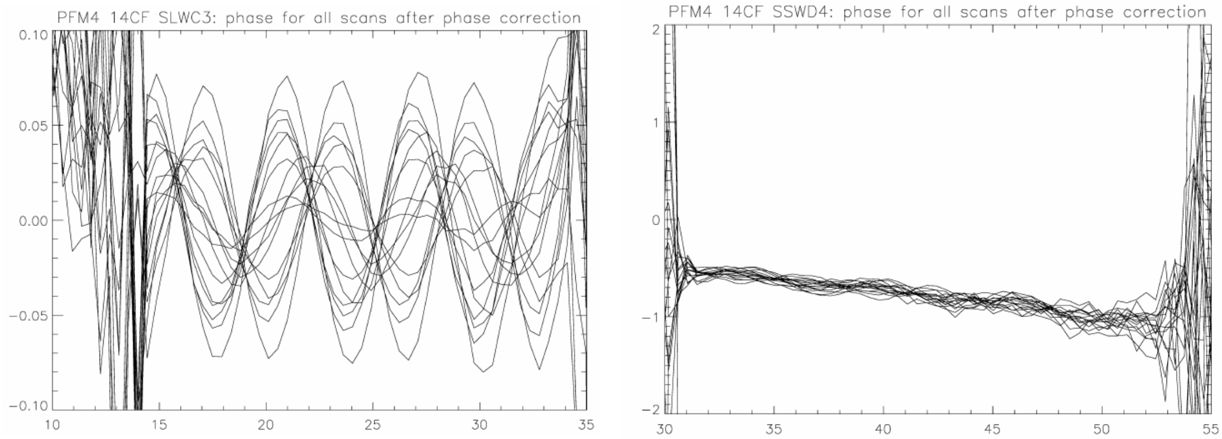

Figure 20: Residual phases in the output data

For SLWC3 one can see that the residual phase, although with a null mean value, exhibits large variations looking like sinewaves. This behaviour has been also found for the runs 30014EC, 30014CE and 30014EB (due to lack of time the results from these runs are not included in the current report). The case of SSWD4 is peculiarly strange as the residual phase seems to have been not corrected at all through the module !!! This behaviour is NOT FOUND in the three other runs to come (30014EC, 30014CE & 30014EB), where the residual phase is very close to zero, with some small sine wave-like oscillations.

My explanation is the following: since the residual phase at the input of the module is not smooth but highly structured (as seen in the attached figures), a fourth order polynomial cannot fit at all the phase within the passband. In the presence of noise the fit can be achieved (nicely!) and the result may be acceptable. In the case of a high SNR I think that the fitting procedure, because of the structure in the phase, does not converge towards a "good" solution but may generate the apparent sine waves. If this is the actual case, then we should consider a phase correction calibration file (a good copy of the phase structure) as the only way to perform the phase correction correctly.

4.6 Apodisation

Tested by David Naylor and Locke Spencer (Lethbridge).

4.6.1 Test Data

PFM4:

OBSID	Date and Time	Mode	Number Scans	Source details
0x300114CA	27/11/06	M	16 Medium	SCal and CBB off

4.6.2 Procedure

Both input and output data were exported from the HCSS environment to be verified externally using IDL. The ratio of apodized to unapodized interferograms (i.e. output to input) was used to obtain the original HCSS apodization kernel. The HCSS kernel was compared to that generated within IDL for the same OPD array. This analysis was performed for 13 apodization functions (Gauss, Hamming, Hann, and 1.1 - 2.0 DN/MT NB apodizations), on both single and double sided (SS, DS) interferograms. Three diagnostics are performed on the data. First, the position of maximum apodization kernel amplitude is verified to be at ZPD. Second, the Mean error is determined, i.e.

$$\text{Mean error} = \frac{1}{N}\Sigma_{i=0}^{N-1}[A_{HCSS}(i) - A_{IDL}(i)].$$

Thirdly, the mean absolute error is determined, i.e.

$$\text{Mean absolute error} = \frac{1}{N}\Sigma_{i=0}^{N-1}[|A_{HCSS}(i)| - |A_{IDL}(i)|].$$

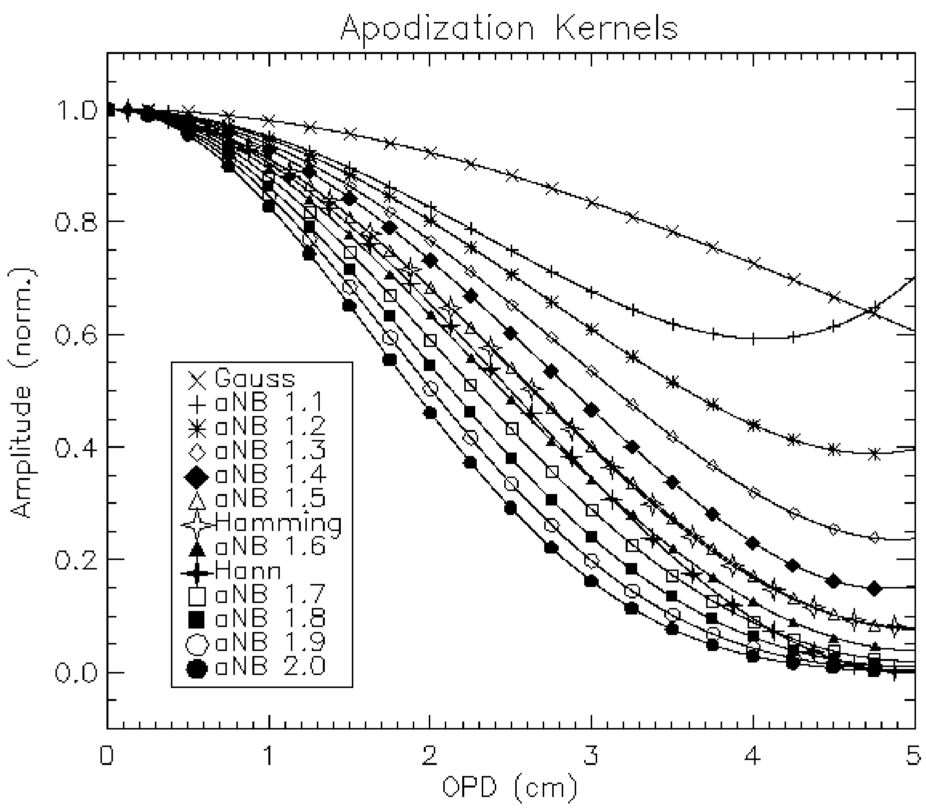

Figure 21: Apodization kernels.

4.6.3 Results

Results are summarized in Table 1 below.

DS /SS	Apodization Function	ZPD (um)	Mean error (%)	Mean abs. error (%)	OBSID	Channel	Scan
DS	1.1	-25	-2.7E-16	1.4E-15	805377226	SLWC3	1
DS	1.2	-25	4.3E-17	1.6E-15	805377226	SLWC3	2
DS	1.3	-25	-2.7E-17	1.4E-15	805377226	SLWC3	3
DS	1.4	-25	-2.4E-17	1.1E-15	805377226	SLWC3	4
DS	1.5	-25	4.8E-17	1.2E-15	805377226	SLWC3	5
DS	1.6	-25	1.8E-16	1.1E-15	805377226	SLWC3	6
DS	1.7	-25	6.4E-17	1.2E-15	805377226	SLWC3	7
DS	1.8	-25	4.8E-17	1.1E-15	805377226	SLWC3	8
DS	1.9	-25	4.2E-17	1.2E-15	805377226	SLWC3	9
DS	2.0	-25	1.1E-16	1.2E-15	805377226	SLWC3	10
DS	Gauss	-25	-2.7E-16	6.6E-15	805377226	SLWC3	13
DS	Hamming	-25	-5.2E-16	1.2E-14	805377226	SLWC3	12
DS	Hann	-25	-9.2E-16	1.3E-14	805377226	SLWC3	11
SS	1.1	0	-1.8E-17	1.4E-15	805378046	SLWC3	1
SS	1.2	0	4.2E-17	1.5E-15	805378046	SLWC3	2
SS	1.3	0	-4.8E-17	1.3E-15	805378046	SLWC3	3
SS	1.4	0	-2.2E-18	1.3E-15	805378046	SLWC3	4
SS	1.5	0	-1.1E-17	1.2E-15	805378046	SLWC3	5
SS	1.6	0	5.5E-17	1.1E-15	805378046	SLWC3	6
SS	1.7	0	-3.8E-17	1.1E-15	805378046	SLWC3	7
SS	1.8	0	-1.3E-17	1.1E-15	805378046	SLWC3	8
SS	1.9	0	9.4E-17	1.2E-15	805378046	SLWC3	9
SS	2.0	0	9.5E-17	1.2E-15	805378046	SLWC3	10
SS	Gauss	0	2.4E-15	4.9E-15	805378046	SLWC3	13
SS	Hamming	0	6.2E-15	8.3E-15	805378046	SLWC3	12
SS	Hann	0	6.6E-15	8.9E-15	805378046	SLWC3	11

Table 1 Apodization verification summary.

The application of the DS apodizing kernel seems to be off by one data point with respect to its highest amplitude occurring at ZPD. The highest amplitude of the DS apodization kernel consistently occurred at -25 µm OPD. This may be related to the ZPD determination routine which we did not directly test in this analysis. It also could be that the DS apodization is shifted by one data point in its application, which should not be the case.

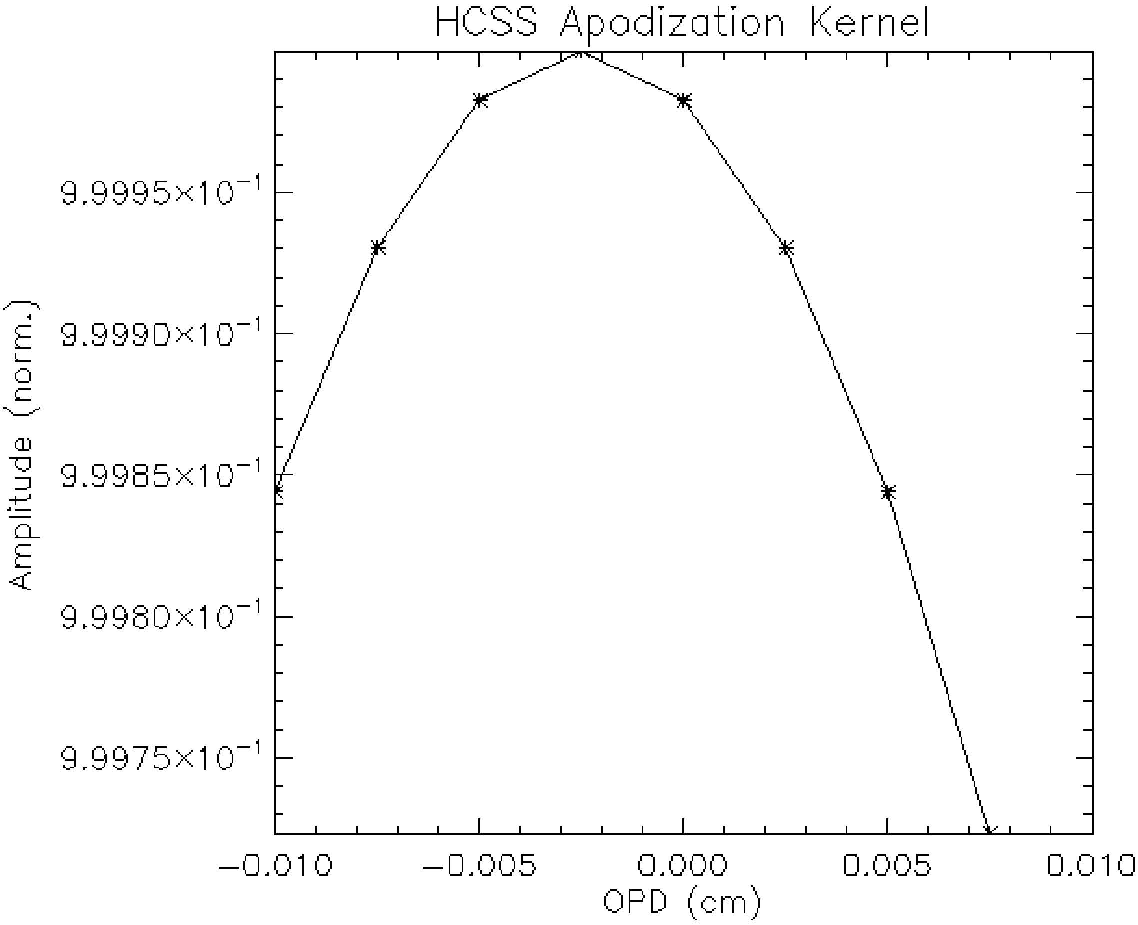

Figure 22: DS apodization ZPD offset.

The edges of the Gaussian apodization were found to be $e^{-0.5}$ in amplitude, corresponding to 1-σ reduction. The Gaussian apodization should truncate at $e^{-1.5}$ in amplitude, i.e. 3-σ.

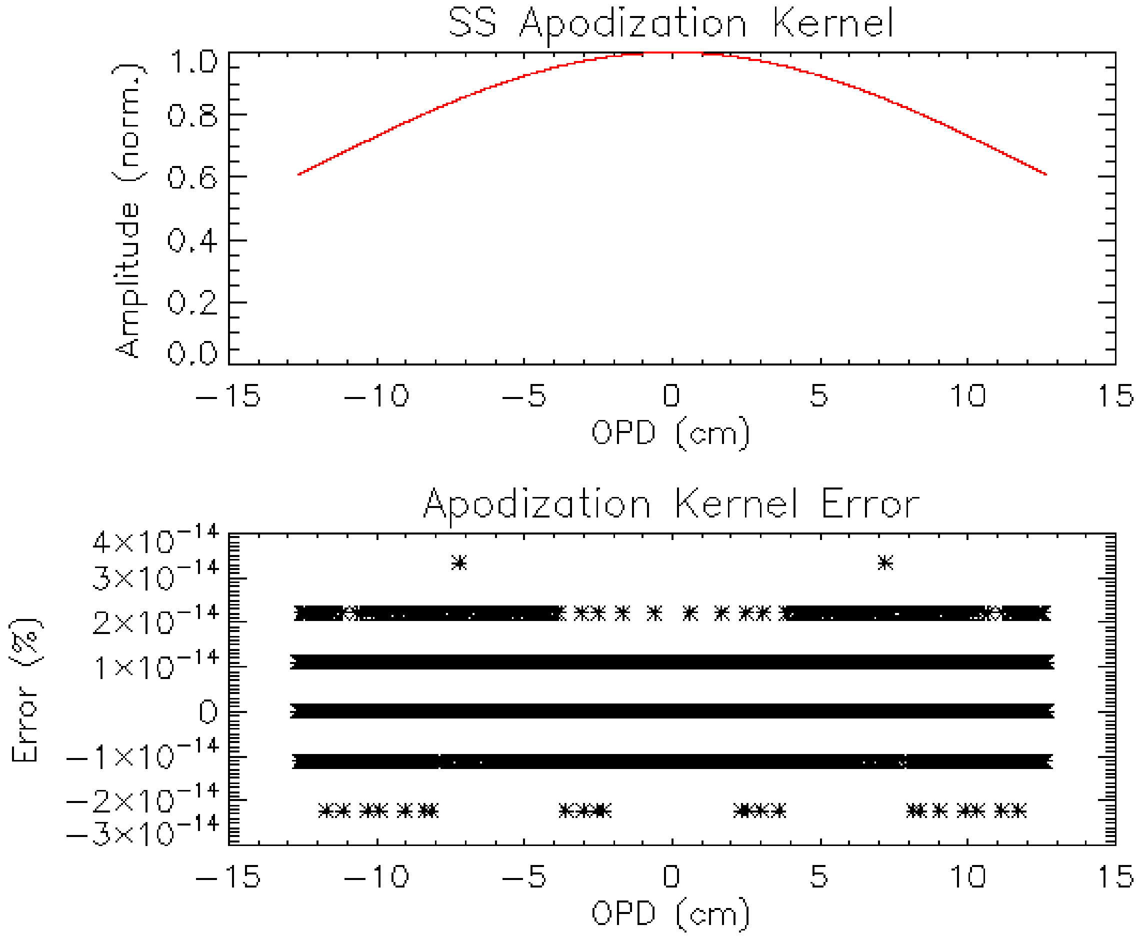

Figure 23: SS Gaussian Apodization

With the exception of the ZPD determination for the DS interferograms, the performance of the HCSS Apodization routine was acceptable.

4.6.4 Mandatory Revisions

1. Fix the point of apodization (i.e. ZPD) for the DS interferogram apodization.

4.6.5 Recommended Revisions

1. Review the desired width of the Gaussian apodization kernel.
2. Insert figure (similar to Figure 1) of apodization kernels into user manual.
3. Reduce the number of available apodizing functions to Hamming, Hanning, Gauss, and the ten adjusted Norton-Beer functions.

4.7 Fourier Transform of Interferogram

Tested by David Naylor and Locke Spencer (Lethbridge).

4.7.1 Test Data

PFM4:

OBSID	Date and Time	Mode	Number Scans	Source details
0x300117FE	8/12/06 18:42-18:50	H	4 High	SCAL4 @ 67.9 K, Laser on SSWD3
0x30011800	8/12/06 19:11-19:24	M	20 Medium	SCAL4 @ 67.9 K, HBB warming up
0x30011801	8/12/06 19:26-19:33	L	40 Low	SCAL4 @ 67.6 K, HBB warming up

4.7.2 Procedure

The inputs, i.e. opd, interferogram signal, and outputs, i.e. wavenumber, real spectrum, imaginary spectrum (where applicable), to/of the HCSS Fourier transform routine were exported for ingestion into IDL for verification. The inputs were Fourier transformed within IDL and the resultant spectra were compared to the HCSS output. The DS FT and SS FT were verified for LR, MR, and HR scans for both SLW and SSW arrays.

Four diagnostics are performed on the data. First, the position of maximum interferogram amplitude is verified to be at ZPD. Second, the difference between the HCSS wavenumber array and the IDL wavenumber array is measured. Third, the Mean error is determined for the real spectrum (DS and SS) and the imaginary and absolute spectra (DS only), i.e.,

$$\text{Mean error} = \frac{1}{N}\Sigma_{i=0}^{N-1}[S_{HCSS}(i) - S_{IDL}(i)]$$

Fourthly, the mean absolute error is determined for the real, imaginary, and absolute spectra where applicable, i.e.,

$$\text{Mean absolute error} = \frac{1}{N}\Sigma_{i=0}^{N-1}[|S_{HCSS}(i)| - |S_{IDL}(i)|]$$

4.7.3 Results

Results are summarized in Tables 2 and 3.

LR /MR /HR	ZPD (um)	WN error (cm-1)	Mean Real Error (%)	Abs. Real Error (%)	Mean Imag. Error (%)	Abs. Imag. Error (%)	Mean Arg. Error (%)	Abs. Arg. Error (%)	OBSID	Chan.	Scan
LR	12.4	4.3E-12	4.3E-16	1.2E-14	2.7E-16	5.4E-15	0.0	0.0	805378049	SLWC3	1
MR	-42.0	4.3E-12	-5.0E-16	1.2E-14	-8.4E-16	1.1E-14	0.0	0.0	805378048	SLWC3	1
HR	-46.8	4.3E-12	-3.7E-16	1.3E-14	-3.2E-15	1.1E-14	0.0	0.0	805378046	SLWC3	1
LR	28.0	4.3E-12	3.1E-16	1.2E-14	2.0E-15	8.7E-15	0.0	0.0	805378049	SSWD3	2
MR	75.8	4.3E-12	3.3E-16	1.6E-14	-6.5E-15	1.7E-14	0.0	0.0	805378048	SSWD3	2
HR	19.7	4.3E-12	-1.1E-16	8.5E-15	1.9E-16	3.0E-15	0.0	0.0	805378046	SSWD3	2

Table 2: Double-sided Fourier transform results.

There is a discrepancy between the uniformly spaced wavenumber array generated with IDL and that given by the HCSS software. This error is smaller than floating point precision as it is shown to be zero when the double precision arrays are converted to floats. This uncertainty is due to OPD sampling non-uniformities and is traced to the observed error through error analysis as follows.

$$\sigma_{Nq} = \frac{1}{2dz}, \delta\sigma_{Nq} = \frac{\delta dz}{2dz^2}$$

The average OPD sampling, *dz*, is determined to be 25.000 000 000 000 001 µm with a standard deviation of 0.000 000 000 002 374 µm. Using the above expression for error in the Nyquist frequency, and the uncertainty of the OPD sampling given by the dz standard deviation, the corresponding uncertainty in the Nyquist frequency is 1.9×10^{-11} cm^{-1}. Since the observed error in the wavenumber grid is less than that determined by the OPD uncertainty by an order of magnitude, the wavenumber error is acceptable.

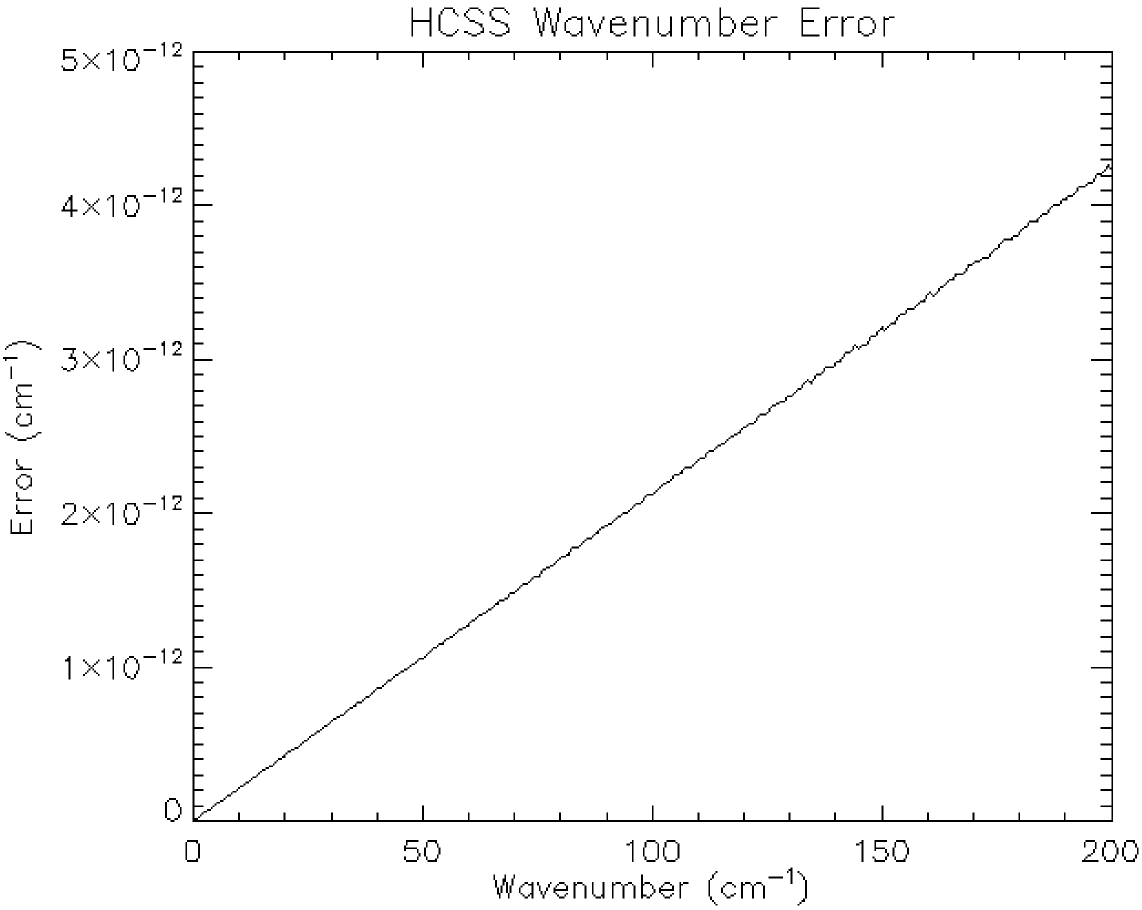

Figure 24: HCSS wavenumber error.

All DS spectra provided excellent agreement between the HCSS and IDL outputs. The real and imaginary errors appear to be due to digital rounding errors within the FT routine. The errors vanish (within double precision accuracy) for the absolute value of the spectra because of the complementarities between the errors in the real and imaginary domains.

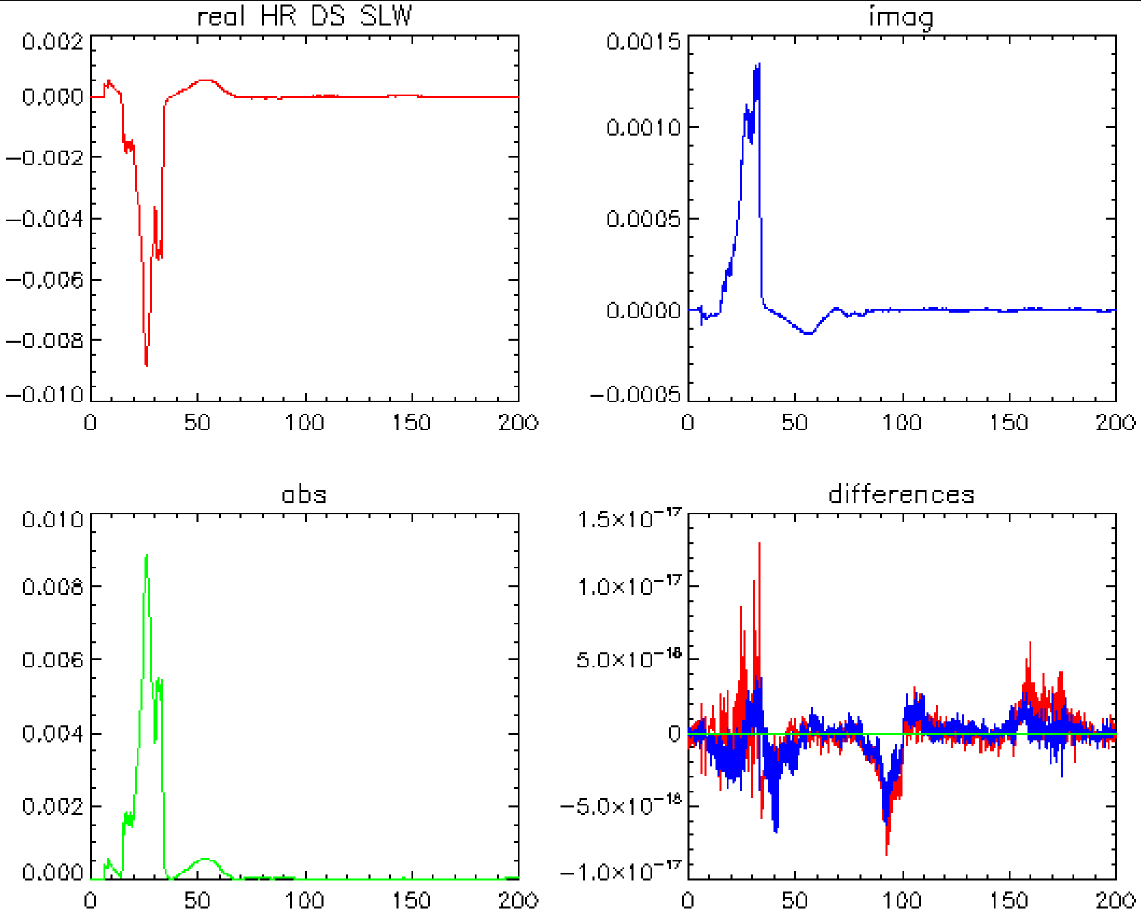

Figure 25: DS FT errors.

LR /MR /HR	ZPD (um)	WN error (cm-1)	Mean Error (%)	Mean Abs. (%)	OBSID	Channel	Scan
LR	12.3	4.26E-12	2.4E-03	1.9	805378049	SLWC3	3
MR	-41.5	4.26E-12	1.9E-12	1.4E-11	805378048	SLWC3	3
HR	-45.7	4.26E-12	1.6E-11	7.8E-11	805378046	SLWC3	3
LR	30.9	4.26E-12	-5.1E-05	0.026	805378049	SSWD3	4
MR	76.1	4.26E-12	-1.6E-12	1.8E-11	805378048	SSWD3	4
HR	71.6	4.26E-12	-6.9E-13	7.1E-12	805378046	SSWD3	4

Table 3 Single-sided Fourier transform results.

The single-sided spectra produced by HCSS are not in good agreement with those generated by IDL for verification. Mean Errors are ~4 orders of magnitude greater than those in the range of $\sim10^{-16}$ as observed for the double-sided Fourier transformation. The spectra themselves appear as if there is a problem with ZPD determination/phase correction, however phase correction was not applied so this is not a concern for this testing. I use the ZPD identified by HCSS and attempt to reproduce the same result.

The HCSS SS LR SLW spectrum appears to have a phase error between the HCSS and IDL generated versions, and is clearly not in agreement with that generated in IDL. All other SS Fourier transform instances are in error, however this error is on the order of ten thousandths of a percentile and is therefore more subtle than the SS SLW LR case.

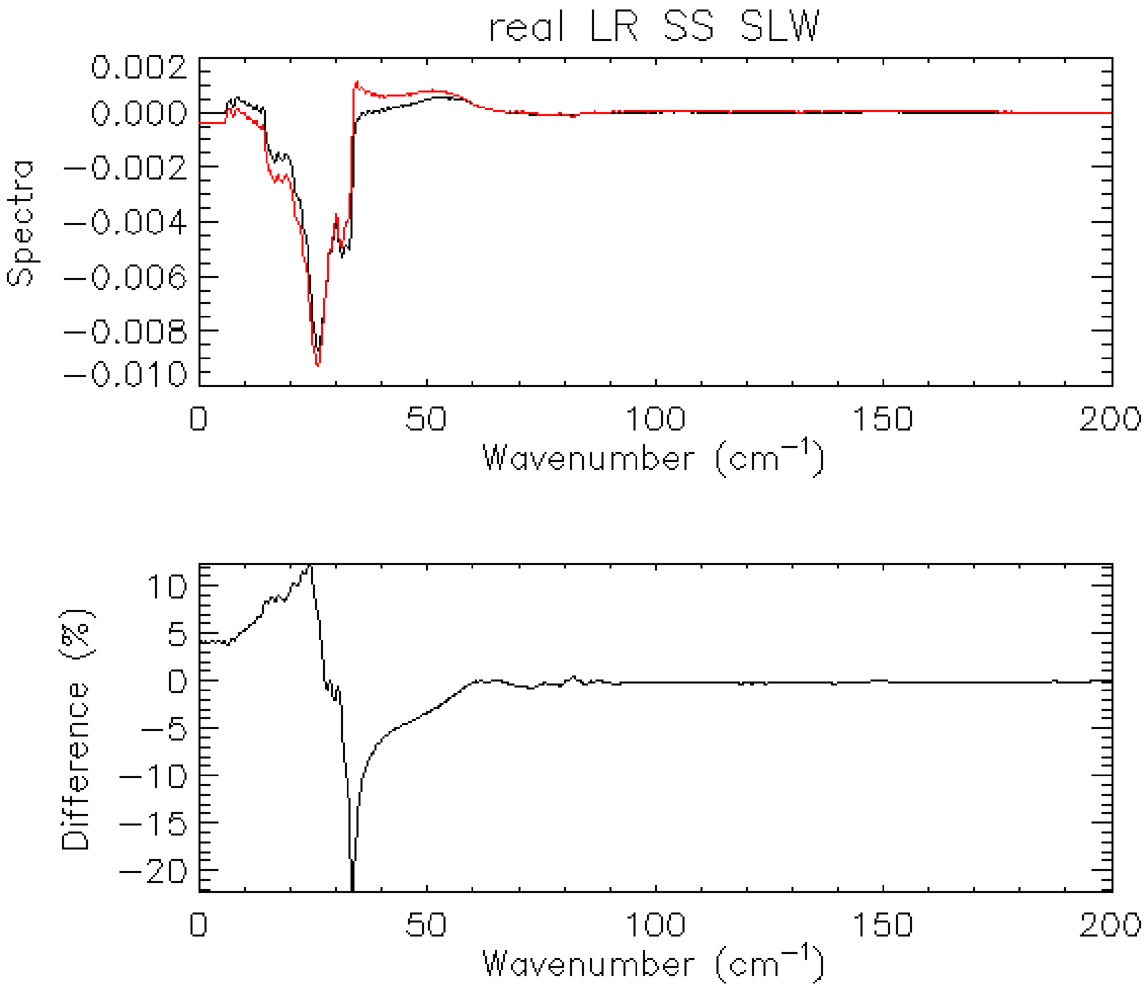

Figure 26: SS LR SLW Spectra.

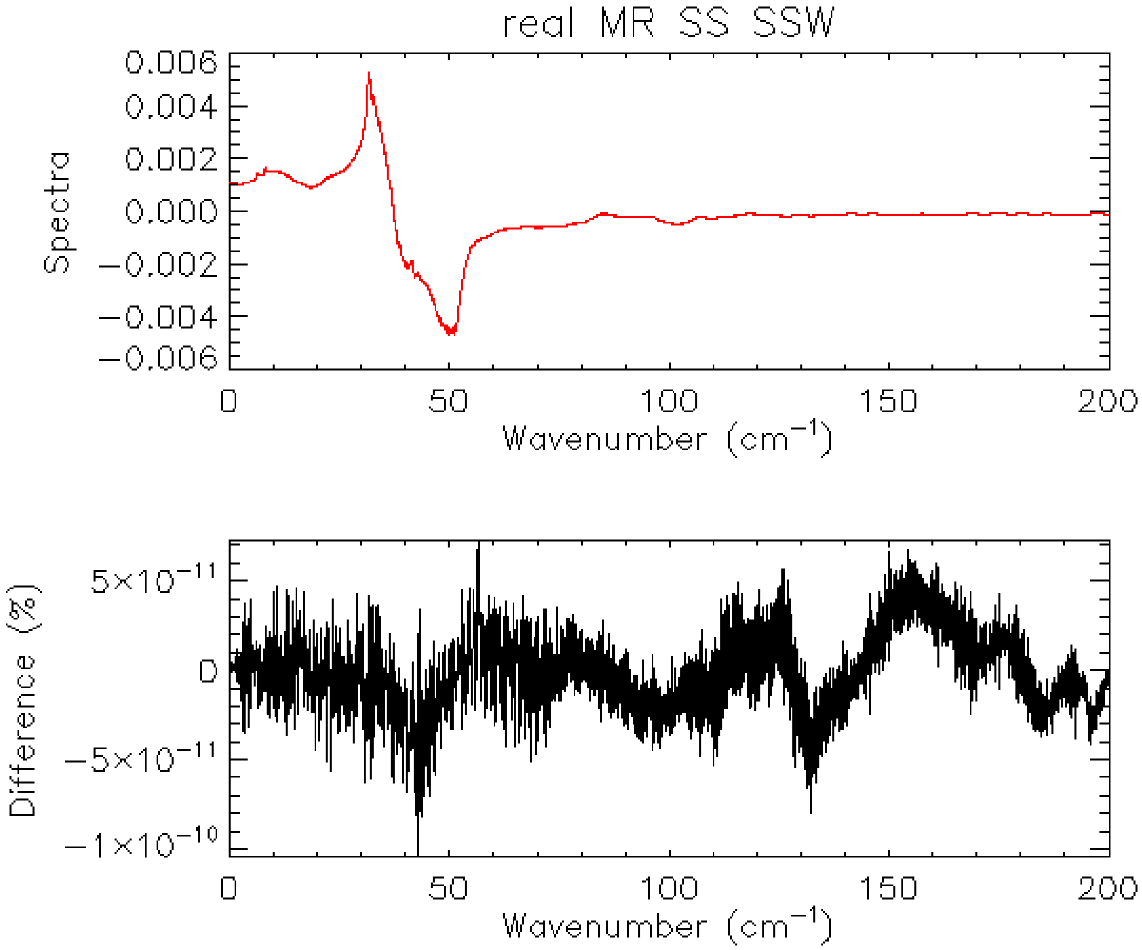

Figure 27: SS MR SSW spectra.

The double-sided Fourier transform performed acceptably for LR, MR, and HR AOTs.

The performance of the single-sided Fourier transform is significantly different between HCSS and IDL. The SS LR SLW case is exceptionally erroneous.

The main difference between the DS FT and the SS FT is the zero padding. The following additional testing is recommended for the HCSS SS FT.

1) Produce LR/MR/HR SS spectra without zero padding for the same observations that we have already looked at and verify the FT.
2) Produce LR/MR/HR spectra where the interferogram has been replaced by the value unity. Verify the FT without and then with zero padding.
3) Using the dat for steps 1 and/or 2 above, pad with zeros such that the data is inflated by an integer multiple, run the FT on both padded and unpadded, and then compare the unpadded spec to the padded spec subsampled by the padding factor.
4) Produce white noise interferograms for LR/MR/HR with/without zero-padding.
5) Using the data from steps 1 and/or 2 above, zero pad to the lengths specified by HCSS (i.e. the 801, 4001, 20001 half lengths), and also the closest power of 2, i.e. the 801->1025 (1600->2048), 4001->4097 (8000->8192), and 20001->32769 (40000->65536). The FFT should work the best with 2^n data points, so this might help identify if something is wrong in the zero padding routine.

4.7.4 Mandatory Revisions

1. Identify the problem with the SS LR SLW Fourier transform.
2. Identify the reason that SS FT errors are ~10^4 times greater than DS FT errors (perform the additional tests recommended above).

4.7.5 Recommended Revisions

1. Review the ZPD determination routine.
2. Review/verify the performance of the Phase correction routine.

4.8 Spectral Averaging

Tested by Nanyao Lu (IPAC).

4.8.1 Test Data

(A)

OBSID	Date and Time	Mode	Number Scans	Source details
0x300114D6	27/11/06 19:54-20:07	H	8 High	SCAL2 @ 9.17 K, CBB off
0x3001172F	06/12/06 15:29-15:42	H	8 High	CBB @ 13 K
0x300117A4	07/12/06 19:28-19:39	L	100 Low	Laser on SLWC3, aperture min

(B)

OBSID	Date and Time	Mode	Number Scans	Source details
0x30012497	05/03/07 17:31-17:53	M	32 Medium	SCAL2 @ 25.2 K

Level-0 telemetry data was downloaded from the RAL PFM4 and PFM5 databases. Calibration files were imported to the LocalStore using “cal_import”.

These tests were carried out using a MacBook Pro with 2G RAM (using Java 1.5).

4.8.2 Expected Results:

Expect that the averaged spectrum confirms the following calculations:

(1) Signal_ave = Sum (Signal_i) / N
(2) Error_ave ^2 = Sum (Signal_i - SignaL_ave)^2 / (N - 1)

where Signal_i is the signal of the spectrum of the i^{th} scan, N = the total number of scans, and the Sum is over the all the valid scans.

4.8.3 General Test Procedures

2) Download the Level-0 data per OBSID from the PFM4 or PFM5 RAL database using obsExporter.

3) Process the data on a per OBSID basis using a Jython script called "test_AVE.py". This script, which is a modified version of the pipeline script SOF1.py, processes the data all the way to the end, but also calculates Signal_ave, and Error_ave directly from individual scan spectra using the formulae above.

4) Compare Signal_ave given by the averageSpectrum module against that calculated directly. No significant difference should be observed.

5) Compare Error_ave given by the averageSpectrum module against that calculated directly. No significant difference should be observed.

4.8.4 Test Results

1) It is true in every test case that no difference was observed in Signal_ave between the module result and the direct calculation. Figs. 28 to 30 show comparisons on some selected channels.

2) It is true in most test cases that no significant difference was observed in Error_ave between the module result and the direct calculation. Figs. 31 to 33 show examples on some selected channels. The only caveat is that, in some cases (c.f. 30012497), there is slight difference on some SSW channels (e.g., SSWA3 in Fig. 31). The differences are still too large to be explained by digitization errors. I did not use the mask information in the direct calculation here. It is not clear to me in the Spectrometer Pipeline Document if any mask information should be used when calculating an average spectrum. So this needs to be further checked out.

My conclusion is that the averageSpectra module is doing what it is specified to do. The only caveat is that we need to determine the source of some minor differences found on the uncertainty calculations on some of the SSW channels.

4.8.5 General Comments on the Pipeline Script SOF1.py:

(1) Why are some channels missing in ASDS (e.g., SLW_C2 in the case of 3001172F)?

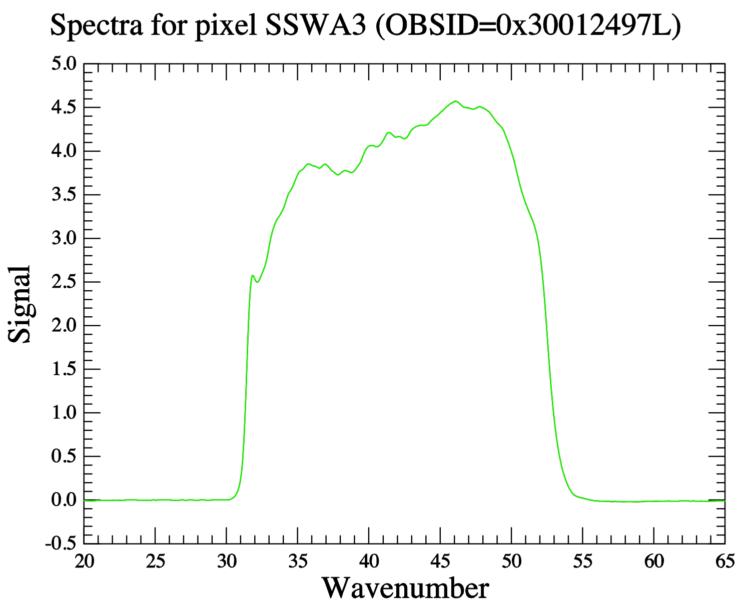

Figure 28: Comparison of the module-produced average spectrum (red curve) with the one calculated directly here (green) on channel SSWA3 in OBSID 30012497.

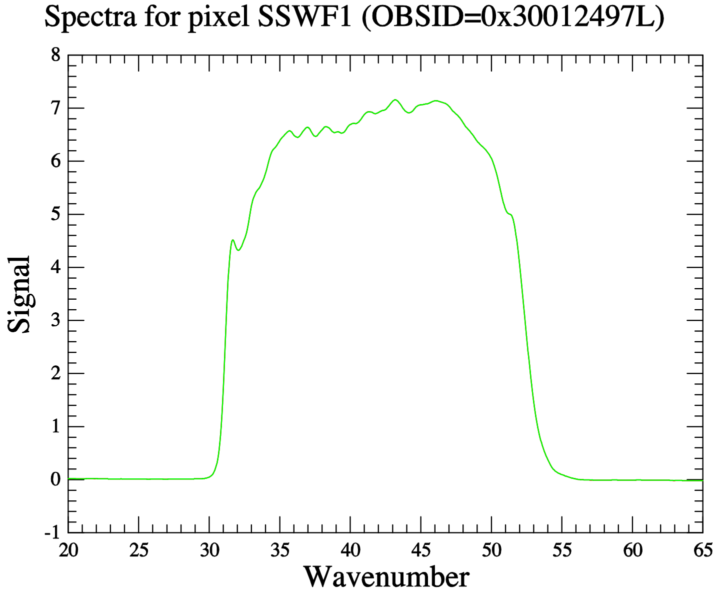

Figure 29: Same as in Fig. 28, but for channel SSWF1.

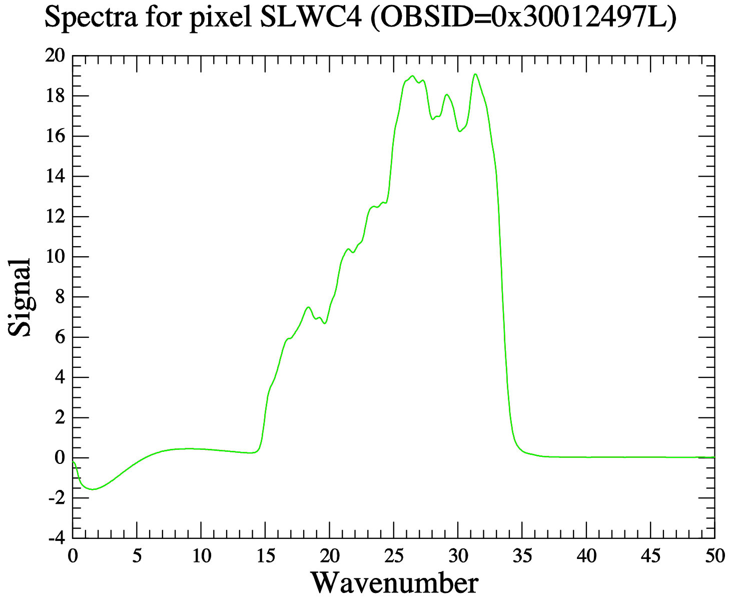

Figure 30: Same as in Fig. 28, but for channel SLWC4.

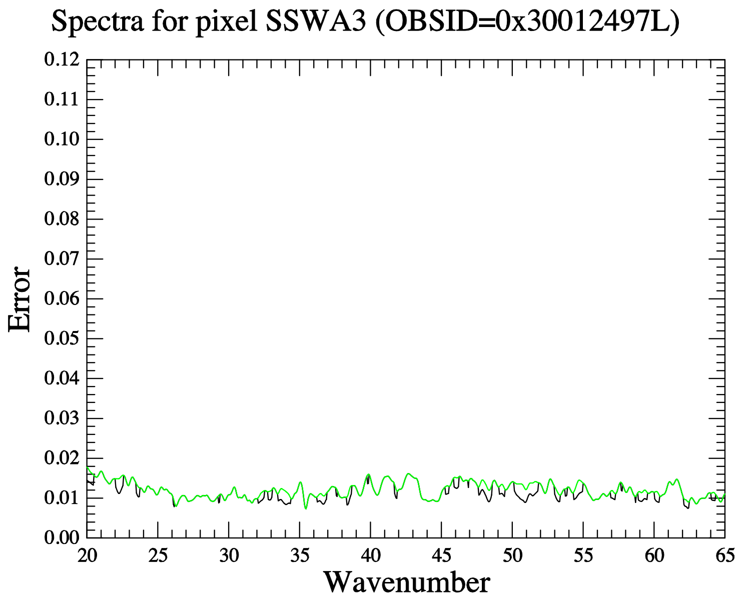

Figure 31: Comparison of the error in the module-produced average spectrum (black curve) with the one calculated directly here (green) on channel SSWA3 in OBSID 30012497. Note some minor differences here.

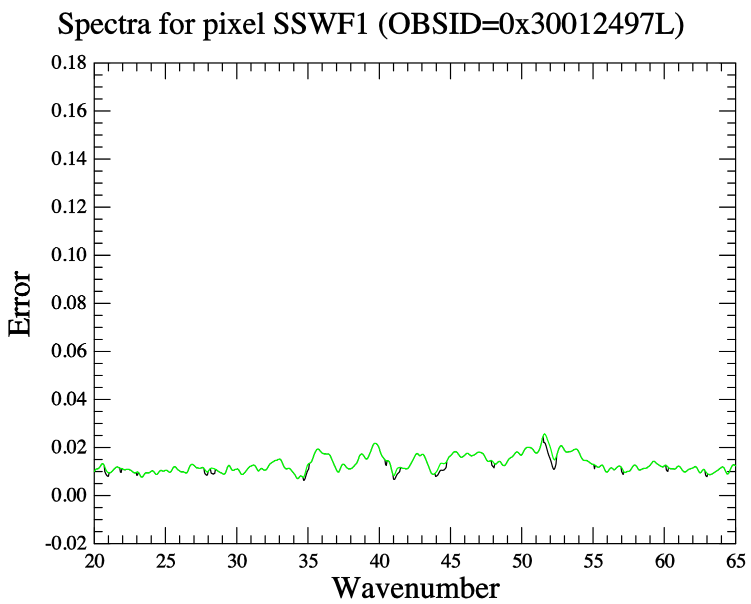

Figure 32: Same as in Fig. 31, but for channel SSWF1.

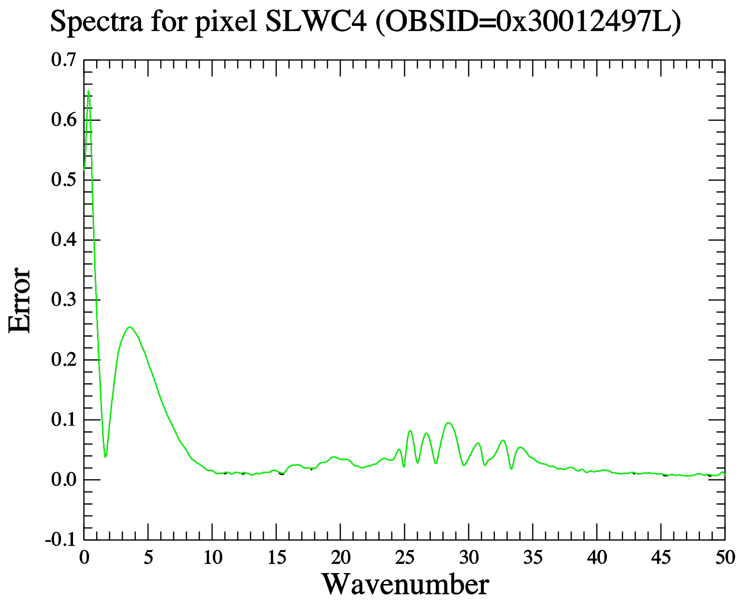

Figure 33: Same as in Fig. 31, but for channel SLWC4.